PHILOSOPHICAL TRANSACTIONS OF THE ROYAL SOCIETY B BIOLOGICAL SCIENCES

How the Dictyostelium Discoideum Grex Crawls

G. M. Odell and J. T. Bonner

Phil. Trans. R. Soc. Lond. B 1986 **312**, 487-525
doi: 10.1098/rstb.1986.0016

Phil. Trans. R. Soc. Lond. B **312**, 487–525 (1986) [487]
Printed in Great Britain

HOW THE *DICTYOSTELIUM DISCOIDEUM* GREX CRAWLS

BY G. M. ODELL[1]† AND J. T. BONNER[2]

[1] *Department of Mathematical Sciences, Rensselaer Polytechnic Institute, Troy, New York* 12181, *U.S.A.*

[2] *Department of Biology, Princeton University, Princeton, New Jersey* 08544, *U.S.A.*

(*Communicated by R. M. May, F.R.S. – Received* 14 *January* 1985)

[Plates 1 and 2]

CONTENTS

† Present address: Department of Zoology, University of Washington, Seattle, Washington 98195, U.S.A.

We propose a new model for propulsion of the *Dictyostelium discoideum* grex (pseudoplasmodium). We concentrate upon the mechanics of the problem: how does each participating amoeba contribute motive force, and how do the myriad force contributions produce a coordinated collective effort?

Experiments we report here show that when a *Dictyostelium discoideum* grex's migration is stalled by mechanically arresting the motion of its boundary, the amoebae in it actively circulate in a reverse fountain flow extending the length of the grex. The velocity of individual cells relative to the grex boundary is commensurate with the migration speed of a grex: approximately one grex length per hour. We argue that cell circulation constitutes the propulsive engine of migrating grexes.

More precisely, we believe each participating amoeba *orients* its attempted motion by the same cAMP chemotaxis used during aggregation. The cAMP concentration field within the grex consists of pulses, emitted periodically at the tip, propagating rearward by the same cAMP relay behaviour seen during aggregation. Existing literature documents chemotactic migration within grexes and generally reinforces the preceding description.

The principal new contribution of this paper is to resolve the following conceptual difficulty: in a close-packed three-dimensional mass of cells, each amoeba trying to crawl can exert traction only upon its neighbours which, in turn, exert traction on it. In the interior of the grex, with no rigid agar substratum to crawl upon, *equal* efforts by a cohort of amoebae to crawl in the same direction, each upon similarly crawling neighbours, cancel and produce no net mechanical result.

In our model of chemotaxis within packed three-dimensional cell aggregates the cells need no rigid substrate. We hypothesize that gradients of other chemicals must arise naturally within grexes, approximately perpendicular to the average cAMP gradient. If one such chemical acts to modulate the traction amoebae exert individually, then a self-regulating, chemotactically oriented, fountain flow of cells must result. We explain how such a fountain can shape and move the grex, and we speculate on the tendency of the fountain to cause the grex cell mass to climb automatically any stalk that might form inside it. Our work thus strengthens the notion, attractive on evolutionary grounds, that a slight modification of the chemotactic behaviour needed for aggregation can account also for the migratory behaviour of the grex and erection of the fruiting body.

In the simplest version of our theory, we assume that regionally differentiated cell types, anterior prestalk and posterior prespore cells, are constantly converting from one to the other. We assume that the grex shapes and moves itself because its constituent cells establish standing chemical gradients, *which remain fixed as seen by an observer riding at the grex tip*. The cells circulate slowly through these gradients and 'act' in a fashion determined by the local chemical environment, so the same cells continuously interconvert between exhibiting pre-stalk and pre-spore type behaviour. Cell circulation through these standing gradients 'rolls' the grex forward.

Of necessity, our formulation is mathematical, phrased in terms of the unfortunately complicated partial differential equations of nonlinear continuum mechanics and spatially heterogeneous reaction–diffusion–convection chemistry. But we give an intuitive discussion, parallel to the essential mathematical one, and show both to predict what we observe experimentally.

1. Introduction

How does an assembly of *Dictyostelium discoideum* amoebae coordinate the behaviour of its constituent cells to function collectively? We are particularly interested in how the characteristic grex shape, polarity, and apparently purposeful locomotion arise. Our fundamental assumption is that the crawling behaviour of a grex is a direct consequence of a set of genetically coded behavioural rules followed identically by each of a myriad participating amoebae. This does not mean that each amoeba would be observed executing the same performance. Each amoeba experiences a different microenvironment, created partly by the behaviour of its neighbours, and therefore responds differently. It does mean that, until stalk formation commences, any amoeba can play any role if given the appropriate external cues.

We do not regard any propulsion scheme to be mechanically feasible if it involves, explicitly or implicitly, an assumption that amoebae in the *interior* of the grex can transmit traction directly to the agar or to anything else fixed with respect to the agar: the slime sheath, for example. Each amoeba can exert traction *only upon* what its periphery *actually touches*. For an amoeba in the interior of the grex, that includes only its neighbouring cells or slime. Only for a monolayer of amoebae located where the boundary of the grex contacts the agar floor, is the slime sheath, stuck to the rigid floor, available to push or pull upon.

We believe this mechanical constraint severely limits grex propulsion possibilities to just four: (i) a layer of amoebae just adjacent to the slime sheath on agar substrate could crawl on it, carrying all others along passively; (ii) without changing neighbours, constituent cells could cause coordinated rhythmic contractions resulting in propagating wavy geometry of the grex boundary which, in turn, could move the grex peristaltically through its slime sheath; (iii) slime exuded at the tip of the grex and absorbed at the tail could propel the grex *without any cell moving at all*; (iv) general fountain circulation of cells within the grex can extrude the grex forward.

PHILOSOPHICAL TRANSACTIONS OF THE ROYAL SOCIETY B BIOLOGICAL SCIENCES

Experimental observations, surveyed in §§3.6 and 6, seem to us to rule out the first three options, while experiments we report in §3 substantiate option (iv).

We explore option (iv) and propose a biologically plausible scheme in which grex locomotion, and even the erection of the fruiting body, results from a variant of the same cAMP chemotaxis that brings individual amoebae to aggregation sites. Roughly speaking, standing gradients of two chemicals arise, and amoebae, whose behaviour is determined by the local conditions they experience, crawl through them causing the grex to 'roll' forward.

We oversimplify and speak as if a grex comprised a population of identical cells. Many experimental observations point emphatically to the possibility that a differentiated subpopulation of amoebae could constitute a propulsive engine that drags the rest of the passive or less active amoebae along. Nevertheless, in building our model in the remainder of the paper, we will assume for conceptual simplicity that the entire grex is an active tractor comprising identically active cells. Once we have a model for such a grex tractor, then we assume this engine can carry passive baggage (other amoebae) either segregated in a trailer or dispersed throughout it, thus diluting it.

For reasons discussed in §6, we believe the latter possibility to be most likely. In the grex, some amoebae are more active mechanically than others; the most active cells, engaged in the kind of cell circulation we model, percolate through the sluggish ones and this leads to a cell fountain engine whose most active participants concentrate toward the tip of the grex. Our preliminary experiments do not quantify the fraction of the amoebae in the grex that participates actively in the fountain flow, but we are certain it is *not* 100%. The preliminary theoretical considerations in this paper forecast the consequences expected if all cells were identically active. Since they aren't, we do not expect quantitative accuracy of our theory. Nevertheless we do expect from our model qualitative insights about the *kind* of cell trajectories to expect in the grex. These serve usefully to guide future experiments that we hope will reveal a quantitatively accurate, global, three-dimensinal description of cell motions responsible for grex locomotion. From such descriptions we hope, ultimately, to extract a quantatively accurate theory.

As will be shown directly, a mathematical model of a grex consisting entirely of one cell type, equally active mechanically, is far from trivial. Although we could formulate our model to account for a heterogeneous cell population, we believe the great complication this entails would obscure more than it reveals.

In §2, we discuss intuitively the profound difference between two kinds of chemotaxis. The first is the well known movement of individual free-living amoebae over a two-dimensional, solid, agar substratum seen during the aggregation phase of the life cycle. The second is chemotactic movement of amoebae through a three-dimensional substratum comprising only slime and crawling amoebae, during which most amoebae never contact any 'solid ground'. Identification of the key conceptual difficulty in the latter case leads to a possible resolution of it, which we describe non-mathematically, but thoroughly.

In §3, we describe experiments we devised to disprove, or partly substantiate, the predictions flowing from §2. These experiments demonstrate clearly the existence of cell circulation throughout the length of the grex. Independent of the theoretical considerations in the rest of the paper, we believe them to disclose important clues about how grexes crawl. In addition, our experimental results coincide with the predictions of the model described in §2.

Section 4 contains a mathematical description of the conceptual model asserted in §2,

PHILOSOPHICAL TRANSACTIONS OF THE ROYAL SOCIETY B BIOLOGICAL SCIENCES

phrased in the partial differential conservation equation language of nonlinear continuum mechanics. This constitutes a new and *general* theory of chemotaxis operating in close-packed three-dimensional swarms of self-propelled microorganisms.

In §5, we simplify and apply the general theory to the particular context of the experiments presented in §3, and describe how the resulting initial, boundary value problem is solved by using a computer. This generates a specific prediction of our model, verified experimentally in §3.

Biologically oriented readers with serious allergies to mathematical equations can safely read up to §4 without encountering one. Those willing to trust on blind faith our claim that §§4 and 5 are correct can safely ignore those sections, for they add only meagre increments in intuitive understanding to the prose descriptions given in §2.

'Descriptions' is a crucial word. The real substance of our concept of how grexes move, the only experimentally testable version, is contained wholly within §§4 and 5. We emphasize that §2 is not a reliable forecast of how our model must behave, but merely describes in words, retrospectively, what actually happened when we formulated our model mathematically and solved its equations numerically.

In §6 we survey and interpret existing experimental literature, some of which supports, and some of which denies, our concept of grex locomotion.

Section 7 summarizes the progress made in this approach toward understanding grex locomotion.

2. A conceptual model for chemotaxis in dense three-dimensional continua of amoebae

2.1. *Chemotaxis steered by a single chemical will not propel a grex*

We wish to avoid mathematical formalities in this section and to communicate intuitively the behaviour of our mathematical model.

During the aggregation phase, amoebae take their direction cues from diffusion wave fronts of a chemical acrasin which they themselves emit. For *Dictyostelium discoideum*, that acrasin is cyclic AMP. In this paper we will refer to the acrasin simply as cAMP. The amoebae orient toward impinging cAMP wave fronts, then crawl in that direction. The details of the mechanisms by which chemotactic perception leads to cell orientation, and by which amoebae exert traction upon the agar floor may be subtle, but the gross mechanical concepts are not. Amoebae are oriented tractors that can crawl over their mechanical surround in a direction determined by chemical cues diffusing through that surround. This phenomenon has been studied extensively, and both continuum differential equation models (see, for example, Keller & Segel 1970; Parnas & Segel 1978), and discrete automaton computer models (see, for example, MacKay 1978) characterize it adequately.

Schaap & Wang (1984) give evidence that pulsatile acrasin waves continue to propagate from the pacemaker tip during the migration or culmination phase, or both, in all species of cellular slime moulds studied so far. These authors assert that the slug's tip forms because the aggregated mass of cells chases the pacemaker cohort chemotactically. Experiments by Matsukuma & Durston (1979), and by Sternfeld & David (1981), show that amoebae in grexes retain the cAMP chemotactic movement ability seen during aggregation. Amoebae in grexes, however, face an apparent dilemma because each must propel itself not upon solid agar, but through a surround consisting of other amoebae trying to propel themselves.

PHILOSOPHICAL TRANSACTIONS OF THE ROYAL SOCIETY B BIOLOGICAL SCIENCES

One way around this difficulty is for the cell population to differentiate so that some amobae (the pre-spore cohort according to current belief) become inactive mechanically and serve as a viscous medium through which the others (the pre-stalk cells) can crawl. This explains the cell-sorting experiments just mentioned, in which one subpopulation of cells, however they may be dispersed initially, congregate at one site, perhaps a cAMP source, in a blob of cells.

If we suppose that a single chemical concentration field (cAMP) guides the locomotion attempts of each cell, as is thought to be the case during aggregation, such a cell-sorting phenomenon would be a one-shot event. Once sorting is complete, no further cell circulation occurs even if active cells continue to strive chemotactically. It is crucial to understand the intuitive reason for this.

Consider a close-packed continuum of cell tractors, each aiming itself by the local cAMP concentration field, and each striving to crawl in that direction with an intensity determined by the same cAMP field. Then, in the vicinity of a given position, all amoebae will have the same orientation and will strive forward with the same intensity. However hard each amoeba strives, there will be no net mechanical consequence, except possibly that due to the boundary layer of amoebae immediately in contact with a solid substrate.

This is demonstrated mathematically in §4, but to see it intuitively, imagine yourself lying in the midst of a close-packed crowd on a flat frozen lake upon which you can gain no traction. You can, however, grasp your immediate neighbours and try to pull yourself forward relative to them. In particular you can rotate yourself to aim yourself in any direction you please. Imagine further that the same single chemical environmental cue orients you and your immediate neighbours, and determines how vigorously each participant attempts to pull himself or herself forward past neighbouring participants. If you crawl on your neighbour at the same speed your neighbour crawls on you, then neither gains relative to the other. When this cancellation of effort is repeated, pairwise, for all neighbours, the result is chaotic local turmoil with no coherent movement in the interior of the crowd. If some participants at the edge of the crowd can grasp the shore (the agar), then they could slide the whole crowd forward, and this corresponds to option (i) in the introduction.

2.2. *The same* cAMP *chemotaxis responsible for aggregation can propel the grex if modulated by a second chemical factor*

A simple modification of our single-chemical steerage scheme can coordinate the futility described above into effective propulsion of the crowd of participants. We hypothesize a heterogeneous concentration field of a second (chemokinesis) chemical which acts not to affect the orientation of cells but to modulate the intensity with which they strive in the direction they are aimed by the cAMP field. Denote by $c(x, t)$ the concentration of cAMP at position x and time t, let $\zeta(x, t)$ denote the concentration of the second hypothetical chemical, and let ∇c and $\nabla\zeta$ denote the gradients of these two chemicals. Suppose that cells experiencing higher concentrations of the chemical ζ strive more vigorously to move in the direction they find themselves aimed. Mathematically, a deficit of a movement-inhibiting factor, of the sort proposed by Durston & Vork (1979), would be exactly equivalent to a surplus of the chemokinesis factor we propose.

To see the consequence of this two-chemical chemotaxis scheme consider the situation sketched in figure 1 in which concentration fields of both chemicals are imposed and held constant, arranged so that ∇c is orthogonal to $\nabla\zeta$. Actually all we need is that ∇c not be parallel to $\nabla\zeta$.

PHILOSOPHICAL TRANSACTIONS OF THE ROYAL SOCIETY B BIOLOGICAL SCIENCES

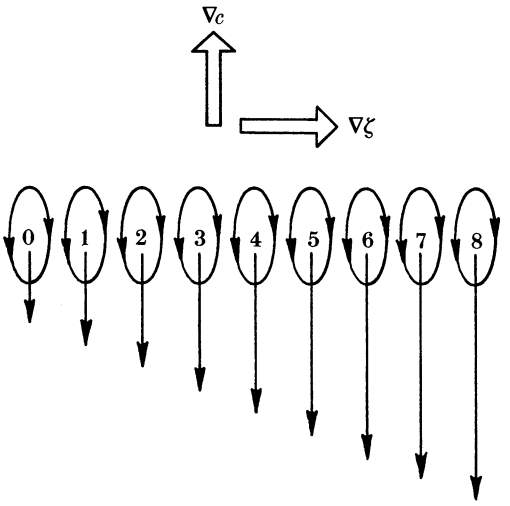

FIGURE 1. The ovals represent individual cells. Each is oriented upwards, in the direction of ∇c. With the concentration of ζ increasing from left to right, the cells on the right strive upward most vigorously because they experience the highest concentration of ζ. The length of the vertical arrow emanating from each cell indicates the intensity with which that cell tries to crawl upward over its neighbours. A shearing flow of cells obviously results because cell 8 'climbs' cell 7 more rapidly than cell 7 climbs cell 6, etc.

Suppose standing gradients of cAMP and ζ can be established and maintained in a migrating grex. A standing gradient is a spatially heterogeneous chemical concentration field which, viewed from a coordinate system attached to the tip of the grex, does not change with time. It can be maintained by a dynamic balance between local production or destruction, diffusion, and convection of the chemical. Also, suppose that in some time-averaged sense the cAMP gradient increases from tail to tip and orients most amoebae to point toward the tip. Finally, suppose that the chemical ζ is a metabolite, produced by all amoebae, and evaporates at the boundary of the grex. This results in ζ having its highest concentration at the mid line of the grex and its lowest concentration at its boundary. Section 6.5 suggests possible chemical candidates for ζ.

We claim (and show mathematically in §§4 and 5) that the assmptions of the last paragraph lead to a continuing self-regulating cell circulation pattern that can propel the grex forward.

2.3. *The movement of amoebae inside a grex whose boundary is immobilized reveals how cells change neighbours to cause migration of a free grex*

Amoebae are nearsighted. We assume an amoeba deep in the interior of a grex has no way to sense directly what other amoebae are doing far away; it senses only chemical concentrations and mechanical events occurring in its immediate vicinity. It cannot, for example, sense its velocity relative to the agar over which it may be moving if the grex to which it belongs is successfully crawling. The way in which the typical amoeba interacts with its chemical environment and its neighbours should therefore not be affected if the motion of the boundary of its grex is arrested by experimental contrivance.

These considerations have two consequences: first, we *can* arrest the boundary of a grex experimentally, as described in §3.1, by a method that makes it easy to measure cell trajectories. Second, our mathematical model's equations can be solved numerically much more easily within a fixed and known boundary than they can when the boundary moves and its position

must be computed. Thus, by assuming mathematically, and forcing experimentally, the grex to have a fixed boundary, we achieve both experimental and mathematical simplicity and facilitate comparison of our theory with experiment.

We now describe the behaviour of our mathematical model in the case of a fixed cylindrical boundary. We consider a continuum of identical amoebae, trapped in a rigid-walled tube. We assume that a constant source of cAMP far to the right and a sink far to the left leads, by diffusion, to a cAMP gradient that varies with x, increasing to the right. Each cell emits the second chemical, ζ, at a fixed rate. This chemical's concentration is assumed to be zero on the sides of the tube. Figure 2 shows what our model predicts after the boundary conditions have

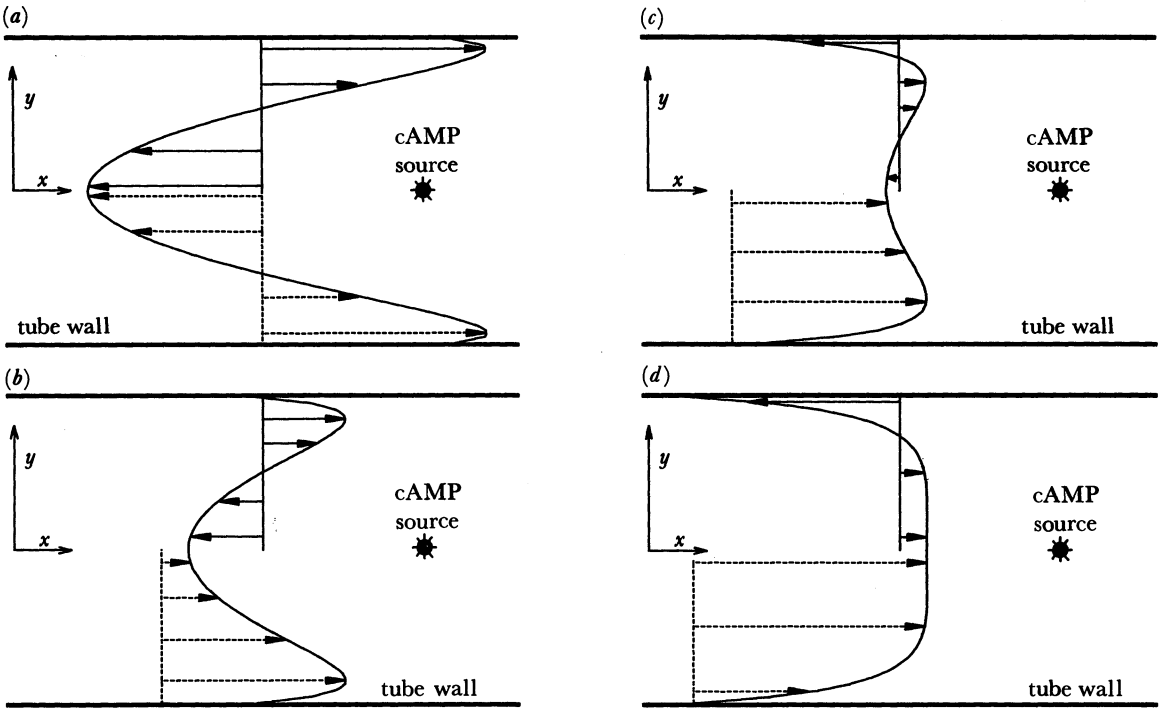

FIGURE 2. Steady-state solutions of the model equations (simplified) for a grex trapped in a rigid-walled 'tube' with plugged ends. For simplicity, the 'tube' is the region bounded by parallel plates of infinite extent. Only the flow far from the tube ends is modelled. A steady cAMP source is assumed to exist, which creates an approximately linear gradient of cAMP rising to the right. Each amoeba generates ζ at a steady rate, and ζ is assumed 0 at the tube walls owing to evaporation of ζ. At higher ζ concentrations, amoebae, aimed along the cAMP gradient, attempt to crawl faster. Initially $\zeta = 0$ everywhere and all cells are at rest. The model equations, derived in §4, are simplified and appropriate boundary conditions are imposed upon them in §5. The solution to these equations is computed numerically and evolves eventually to the steady-state shown in the figure. The ζ concentration profile (not shown) is parabolic, highest at the centreline of the tube. The mass-averaged velocity field can be proved to point parallel to the tube's axis, and very only with distance, y, from that axis.

In each panel the mass-averaged velocity profile, $V(y)$, is shown graphically. The solid arrows in the upper half of each panel indicate cell velocities seen from a coordinate system attached to the tip (that is, moving at the net axial speed of the entire cell mass). The dashed arrows in the bottom of each panel indicate cell velocities seen from the lab coordinate system fixed with respect to the tube walls.

Panel (*a*) shows the completely reversed fountain flow predicted when the ends of the tube are plugged precluding *net* forward flow ($R = 0$ in §5).

As the force acting at the front end of the tube to prevent forward motion diminishes successively in panels (*b*) ($R = 0.25$), (*c*) ($R = 0.75$), and (*d*) ($R = 2.00$), the model predicts that the region of flow reversal (as seen from the tip coordinate system in which *net* axial flow is always zero) shifts from the core to zones near the tube walls.

been enforced for a long time and the solution to our equations approach their steady-state solutions. Refer to the caption of figure 2 for details, and to §§4 and 5 for the formal mathematics leading to the results shown. The four panels in figure 2 show predicted behaviour of the model as the force opposing net movement of the cell mass down the tube decreases from infinite (in 2*a*) toward inconsequential (in 2*d*). Figure 2*a* corresponds to the imprisonment experiment described in the next section.

The outcome shown in figure 2*a* may seem counterintuitive; the cells on the axis of the tube experience the highest concentration of the chemical ζ and therefore strive most vigorously forward. Nevertheless, these cells are driven backwards (to the left) opposite to the direction in which they try to crawl. The farther a cell is from the tube axis, the lower the concentration of ζ it experiences and so the less vigorously it strives. Yet cells near the tube walls, which are not trying, individually, nearly as hard as are those at the axis, flow forward, overpowering those at the axis. The $\zeta(y)$ field has an extremum at $y = 0$, so the most vigorous cell of all, the one at $y = 0$, makes no progress whatever simply because its nearest neighbours are crawling on it just as vigorously as it crawls upon them; their efforts cancel. Where the gradient of ζ is steepest, namely near the tube walls, each cell crawls over its neighbour nearer the wall significantly faster than that neighbour crawls on it. An active shear flow of cells results and pushes a river of cells foward near the periphery of the tube. Since, in figure 2*a*, the ends of the tube are plugged, one cell can move forward only if another moves backward. Thus, the forward currents near the periphery force a backward current which turns out to be concentrated near the tube's axis. In the mathematical model, flow reversal in the central core is caused by *stalling* the grex. The greater the impediment to forward flow is, the more pronounced the flow reversal is. With sufficiently small resistance to forward flow, backward cell flow (as seen from the tip coordinate system) occurs near the tube walls, not near the core (cf. figure 2*d*), according to our model.

2.4. *Our model may explain the mechanism by which a grex elongates out of the hemispherical aggregation mound*

The discussion in §2.3 assumed existence of a cAMP source at the tip, and assumed the grex had already acquired its cylindrical shape. We believe our model can account both for the initiation and for maintenance of these features, starting from the hemispherical aggregation mound as follows: we assume that during aggregation a small cohort of cells, centrally located, become cAMP signalling pacemakers. That is, they periodically emit pulses of cAMP that, by diffusion, trigger surrounding cells to relay similar pulses and crawl toward the central pacemakers. Suppose this central cohort continues autonomous cAMP pulse emission after aggregation is complete. Figure 3*a–c* show a top view of the situation. The caption describes how we expect participating amoebae, that aim up the cAMP gradient and crawl at a speed modulated by the chemical ζ, to push the pacemaker cohort to the nearest periphery of the aggregation mound and keep it there. In the process, they will extrude the mound into the long cylindrical shape called a grex. In this view the tip steers the migration of the grex because, when the tip emits cAMP pulses, the rest of the amoebae chase it forward into its continuing position of apparent leadership.

PHILOSOPHICAL TRANSACTIONS OF THE ROYAL SOCIETY B BIOLOGICAL SCIENCES

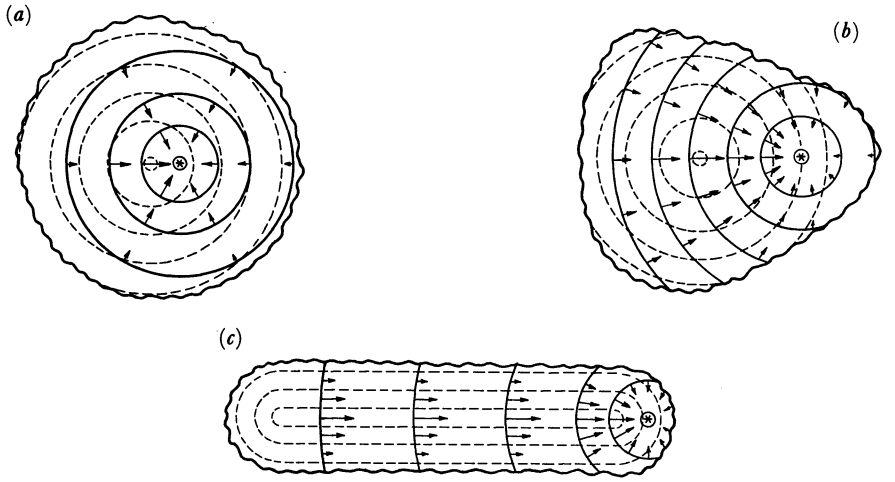

FIGURE 3. This figure illustrates the behaviour expected intuitively from our model when applied to an initially circular mound of cells, shortly after the completion of aggregation. In each picture, the pulsing cAMP pacemaker cells are indicated by an asterisk. Solid lines show concentric constant cAMP loci surrounding this source. Cells orient perpendicular to these lines in the direction of ∇c. Dashed lines show constant ζ loci, with highest ζ concentration near the centre of the cell swarm. $\zeta = 0$ on the boundary of the cell mass, which is shown by a wavy solid line. The arrows represent the orientation of amoebae and the lengths of the arrows are proportional to the intensity with which amoebae attempt to crawl (determined by the concentration of ζ).

In (*a*), we imagine the cAMP pacemaker source to be slightly to the right of the centre of the cell mass. As indicated by the arrows, amoebae to the left of the cAMP source attempt to crawl more vigorously than do those to the right, and this should result in the cAMP source being chased toward the nearest boundary of the mound. The figure shows a two-dimensional caricature. In the real three-dimensional situation, no off-centre location of the pacemaker is necessary initially because an exactly centred pacemaker would be chased vertically upward.

In (*b*), the distance between the zones of highest cAMP and ζ concentrations has been increased, and this amplifies the dominance of the cells to the left of the cAMP source, accelerating the tendency of amoebae to chase this source to the periphery.

In (*c*), the cAMP source has been chased into its leadership position at the tip and the mass of amoebae, all striving to reach the tip, has elongated into a cylinder. In this configuration the gradients of cAMP and of ζ are nearly perpendicular throughout most of the cylinder, and this maximizes the tendency of the cells to generate active shearing flow. Our expectation is that the cylinder will not elongate indefinitely because smaller diameters mean lower concentration of ζ and thence less vigorous attempts by participating cells to crawl. This means an equilibrium length:diameter ratio should be maintained, but we do not know what that ratio might be because we have not yet actually solved the equations applied to the situation shown.

Note that the reasoning illustrated in this figure leads also to the expectation that, if several cAMP sources were present and separated sufficiently initially, then they should be chased to different regions of the periphery, and then maximally separated. This could explain how surgically implanted extra tips lead off contingents of cells from one grex to form two. It could also explain the multiple miniature fruiting bodies that radiate from the blobs of cells left along the stalk as *Polysphondylium* culminates.

2.5. *Our model may account for the irregular tip pulsations seen in time-lapse films of migrating grexes*

The boundary value problem posed and solved in §5 does not account for how cells reverse their directions at the tube ends, but, whenever the net forward motion is partly stalled as in figure 2*a*, *b*, something resembling the flow shown in figure 4 should occur. That is, a reverse fountain circulation at the tip is consistent with the solution computed. Since we have not yet done the difficult computations needed to solve the appropriate boundary value problem using our model's equations, we are not certain that our model actually accounts for such a reverse fountain at the tip.

The issue most in doubt concerning the behaviour at the tip is this: will the cohort of cAMP

pacemaker cells be kept stably in the tip as an automatic consequence of the rest of the amoebae chasing it? Intuitively, the position of the pacemaker cohort at the stagnation point of a reverse fountain would seem to be a stable one radially and a possibly unstable one axially. That is, referring to figure 4, if the pacemaker cohort were accidentally displaced off centre in the y (radial) direction, the reverse fountain flow would push it back to the centre. On the other hand, if the pacemaker cohort is displaced slightly axially away from the tip, the reverse fountain flow would carry it further backward down the core of the grex. This may be a virtue of our model rather than a flaw. Whenever the pacemaker cohort is swept backward away from the tip, it would cease temporarily to organize the rest of the cells to form the reverse fountain and induce them instead to chase the pacemakers back to the tip, as explained in the preceding subsection. The observed result would be axial mechanical pulsations of the tip as the pacemaker continually loses, then regains, its leadership position at the tip. Saltatory motion of the grex tip is, in fact, a prominent feature observed in time-lapse movies of migrating grexes.

Flows with forward cell fountains, as in figure 2*d*, would seem to create streamlines at the tip that would prevent the pacemaker from residing stably at the tip.

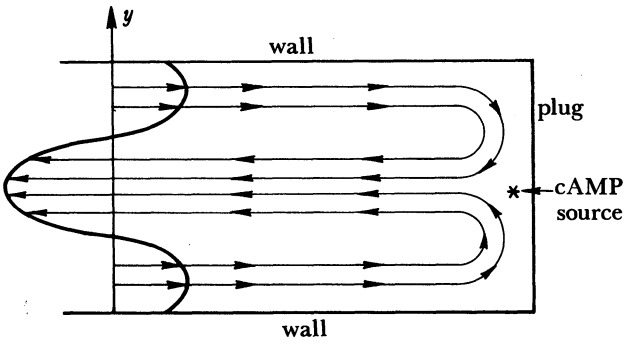

FIGURE 4. This shows conjectured flow reversal streamlines at the tip end of the tube consistent with the simplified boundary value problem solution shown in figure 2. Cells at the tip would move as in an invagination, or 'reverse fountain'. In this artificial rigid-walled boundary problem, no tip shape can be predicted because we have *imposed* a square tip shape.

2.6. *What does a reverse fountain in an imprisoned grex tell us about locomotion of a free grex?*

What happens when the grex is contained not by an agar prison but merely by its slime sheath? In §5 we compute the axial pressure gradient, increasing from left to right, needed to stall the forward movement the grex attempts when imprisoned. This gradient, multiplied by the length of the grex, is the elevation of hydrostatic pressure at the grex tip above that at its tail. This pressure excess multiplied by the cross-sectional area of the grex is the force the anterior cap of the slime sheath would have to sustain to stall the grex. When the slime sheath plays the role of the prison walls, it may be unable to withstand this force. Then this force could 'roll out' the slime sheath at the tip. In §5, we assume the force needed to 'roll out' the slime sheath is proportional to the rate at which the sheath is rolled out. The axial pressure gradient needed to slow the advance of a grex down a tube increases the more the grex is slowed. In the simulations described in §5 and shown in figure 2, the grex 'rolls' forward at just that speed at which the impeding force of the slime sheath balances the pressure force at the grex tip needed to slow the cell fountain to that speed, and a partly reversed cell fountain can result.

PHILOSOPHICAL TRANSACTIONS OF THE ROYAL SOCIETY B BIOLOGICAL SCIENCES

The less force needed at the tip to roll out the slime sheath, the faster the grex crawls, and the less apparent is the reversal of the cell fountain. In fact, when the slime sheath offers sufficiently little resistance to the forward shear flow of cells, the fountain does not reverse, but runs so that, seen from a coordinate system at the grex tip, the cells in the central core move forward while those on the periphery touching the agar go backward: the opposite (in figure 2*d*) of what is depicted in figure 2*a*.

Subsections 2.4, 2.5, and 2.6, contain speculation on issues we will attempt to resolve rigorously in a future publication.

3. Both imprisoned and free grexes exhibit global cell circulation

3.1. *How to make a prison for a grex shaped exactly like the grex's natural boundary*

A liquid droplet of agar at a temperature of 41 °C, dropped upon a freely migrating grex, gels so quickly that it imprisons the grex in a chamber congruent to the grex's natural boundary. Neither the heating nor the diminished oxygen tension the grex suffers consequently seems to interfere with its attempts to develop normally. Grexes remain so vigorous that they often burst free of the prison. The grex will extrude itself backward out of the prison through any remnant of a lumen in the slime sheath. Thus the sheath must be severed before the imprisoning agar droplet falls. Grexes that remain trapped eventually commence stalk formation, always starting it at the original tip end.

The transparent agar prison not only eliminates the reflections cast by the surface of a freely wandering grex but also eliminates the continuous need to re-focus the microscope to track a moving target. A motionless boundary eliminates the chore of delineating cell motions caused by boundary deformations and by local cell–cell interactions. If any amoebae stained with neutral red dye move within the prison, it is easy to record their trajectories by timed sequences of photographs. We assume the conditions stated at the beginning of §2.3. hold in this experiment.

3.2. *Imprisoned cells stained with neutral red vital dye exhibit reverse fountain circulation*

We made cell trajectories visible by transplanting small cohorts of cells from a grex stained throughout with neutral red dye into an initially unstained grex. Red cells were transplanted from the posterior and anterior ends of donors into the same locations in the recipient just before imprisoning the recipient. We then made colour 35 mm slides of the imprisoned grex at 2 min intervals at 25 × magnification. Some of these photographs are shown in figure 5, plate 1.

Stained posterior cells moved toward the tip in a river near or at the periphery of the trapped grex. Stained anterior cells moved posteriorly. Our data show the three-dimensional grex projected into a two-dimensional photograph and so they do not prove this rearward motion occurs near the core of the grex. However, by gauging cell depth from the microscope focal plane, we believe this to be so.

The visible macroscopic circulation of cells demonstrated in this experiment confirms qualitatively the prediction made in §2, shown in figure 2*a*. We cannot conclude more from this preliminary experiment because we do not know what cAMP gradients the imprisoned grex may have generated. At 25 × magnification, we cannot discern the orientation of amoebae. We do conclude, from the fact that the imprisoned grex shown in figure 5*a* commenced stalk

PHILOSOPHICAL TRANSACTIONS OF THE ROYAL SOCIETY B BIOLOGICAL SCIENCES

formation about 8 h after being imprisoned at its original tip end, that the grex did not reverse its original orientation. We have no experimental information about distributions of the hypothetical chemical ζ.

3.3. *In freely migrating grexes, the fountain may not reverse*

As explained in §2.6 and in the caption to figure 2, we expect our model to predict a reversed fountain, as illustrated in figure 2*a*, only when the forward progress of the grex is blocked, by a stiff slime sheath or agar prison walls, for example. In freely migrating grexes, the cell circulation in the core may be only partly reversed or not reversed at all. The frames of figure 5*b* show the cell flow we observed when a stained posterior graft was implanted in the posterior of a clear grex. The stained cells streaked forward, reaching the tip in about 45 min. Note that, while the whole grex is moving forward relative to the agar, the red cells are moving forward relative to the tip of the grex. By adjusting the microscope focal plane up and down, we believe the posterior to anterior cell flow marked by the neutral red dye occurred near the central region of the grex, not at the periphery as happens in an imprisoned grex. The forward movement of the stained cells up the core from their posterior injection site corresponds exactly to the model's predictions shown in figure 2*d*.

We stress that the strking difference between the fountain flows predicted by our mathematical model in figure 2*a* (backward flow in the core) and figure 2*d* (forward flow in the core) is due only to a lowered resistance to forward net motion in figure 2*d*. Removal of the prison's constraint of net forward motion is, likewise, the only difference between the experiments shown in figure 5*a*, *b*.

3.4. *The tail-to-head circulation time correlates with the time it takes a grex to move one of its own lengths*

The stained posterior cells transplanted to the posterior end took approximately 45 min to move to the anterior tip of the imprisoned grex. This statement is true equally of free and imprisoned grexes. We emphasize this because that is the approximate time a 1 mm long grex takes to travel one of its own lengths. In other similar experiments (not shown) with grexes approximately 1 mm long, posterior cells sometimes travelled to the tip within 15 min, but never took longer than 1 h.

3.5. *The peripheral amoebae in the grex can climb up a solid or a liquid core of cells*

We have the following view of the locomotion of a grex: a central core of cells is climbed by amoebae in the periphery. Seen from a coordinate system riding at the tip of the slug, this core moves backward while the 'climbing' cells move forward and this forces the reverse fountain flow at the tip.

Normally in a young grex, the core would be relatively fluid rows of cells. Sometimes, as culmination approaches, it is possible to show, by disrupting the slug with a fine glass needle, that there is a stiffer core: no doubt the precursor of the stalk proper. Indeed, in most species of slime moulds, a stalk is formed continuously during migration, so that a rigid core is always present to be climbed horizontally, just as it is present during culmination in *Dictyostelium discoideum*.

In the migration of the grex, the more rigid the core, the more effective the propulsive engine. But our mathematical model, discussed intuitively in the preceding section, shows the

PHILOSOPHICAL TRANSACTIONS OF THE ROYAL SOCIETY B BIOLOGICAL SCIENCES

mechanism can work even when the core is completely fluid, comprising crawling amoebae. Semisolid cohesiveness in the core makes an even better central strut for the surrounding amoebae to 'climb'. Of course, for vertical erection of the fruiting body into air, it is essential to have a truly solid central strut.

It is tempting to speculate that the gradually stiffening core we believe we find in ageing *Dictyostelium discoideum* grexes comprises amoebae in imminent risk of turning irreversibly to stalk. The chemical environment maintained by standing gradients in the central anterior core may induce the cells crawling through it to become stalk. If these amoebae circulate rearward and to the periphery, however, they enjoy a different chemical environment, and get a temporary reprieve from the self-sacrifice some cells must make eventually to build stalk. *Dictyostelium discoideum* amoebae may differ from the majority of slime mould species, which make stalk continuously during migration, simply by being more hesitant to turn irreversibly to stalk under the influence of the anterior core chemical environment.

3.6. *Do these experiments confirm our theory? Is the chemokinesis chemical really necessary?*

Suppose no chemokinesis chemical with a radial gradient operates. Suppose every cell attempted to crawl axially with the same traction as every other cell. Then arguments in §§2.1 and 4.2 show that no shear flow of cells can be generated by interaction of cells inside the grex. Those arguments ignore tractions exerted at the outer boundary of the grex. Obviously, any viscous fluid can be churned about by stresses exerted at its boundary. The cells at the boundary of the grex contact the slime sheath and can transmit force, through it, to the surrounding agar. In other words, option (i) in §1 could explain grex locomotion.

In an imprisoned grex, the boundary cells could crawl foward only if others move backwards. If *any* mechanism pushes the outer layer of cells forward, then a compensating reverse flow in the core must result. Cells in contact with the prison walls could provide that mechanism. An absence of cell circulation in an imprisoned grex would, of course, disprove our theory. However, the forward motion we observe near the boundary of an imprisoned grex does not prove that a chemokinesis chemical is needed nor does it prove that our explanation of our experiments is correct.

Description of plate 1

Figure 5. (*a*) A sequence of photographs of an imprisoned grex following surgery to transplant stained posterior and anterior cell masses from homologous locations in a donor. The posterior is to the left. The vertical bar to the far left is a cut made through the slime sheath before imprisonment under agar. The circle at the upper right is a landmark useful during digitization made by sticking a hole in the agar. The photographs were made at the following times after surgery: (i) at 16 min, (ii) at 24 min, (iii) at 30 min, (iv) at 39 min, (v) at 61 min, and (vi) at 77 min. Unfortunately, there was an air bubble in the agar toward the anterior end of the grex, and the grex moved slightly forward to fill up the bubble. The pronounced forward movement of posterior cells along the grex periphery, and the simultaneous rearward flow of anterior cells down the core matches the predictions of our model shown in figure 2*a*. Note the pronounced reverse fountain in the tip. The imprisoned grex is about 1 mm long.

(*b*) A sequence of photographs of a freely migrating grex, at (i) 8 min, (ii) 25 min, (iii) 30 min, and (iv) 42 min after a neutral-red-stained graft of posterior cells was implanted in the posterior. The posterior end is toward the left. A graft of stained anterior cells was implanted in the tip. Cell circulation in the tip homogenizes the stain in the tip before much directed cell motion can be detected. As the grex crawls forward, the posterior graft remains coherent, however, and streaks forward (relative to the moving grex), reaching the tip within about 40 min. Here, by gauging the position of the posterior–anterior red cell stream by using optical sectioning techniques, we believe the cells move anteriorly up the axis of the grex, not up the periphery as in the case of trapped grexes. These observations match the simulation shown in figure 2*d*. Evidently the slime sheath offers too little resistance to stall and reverse the cell fountain. The slug began culmination about 70 min after surgery.

PHILOSOPHICAL TRANSACTIONS OF THE ROYAL SOCIETY B BIOLOGICAL SCIENCES

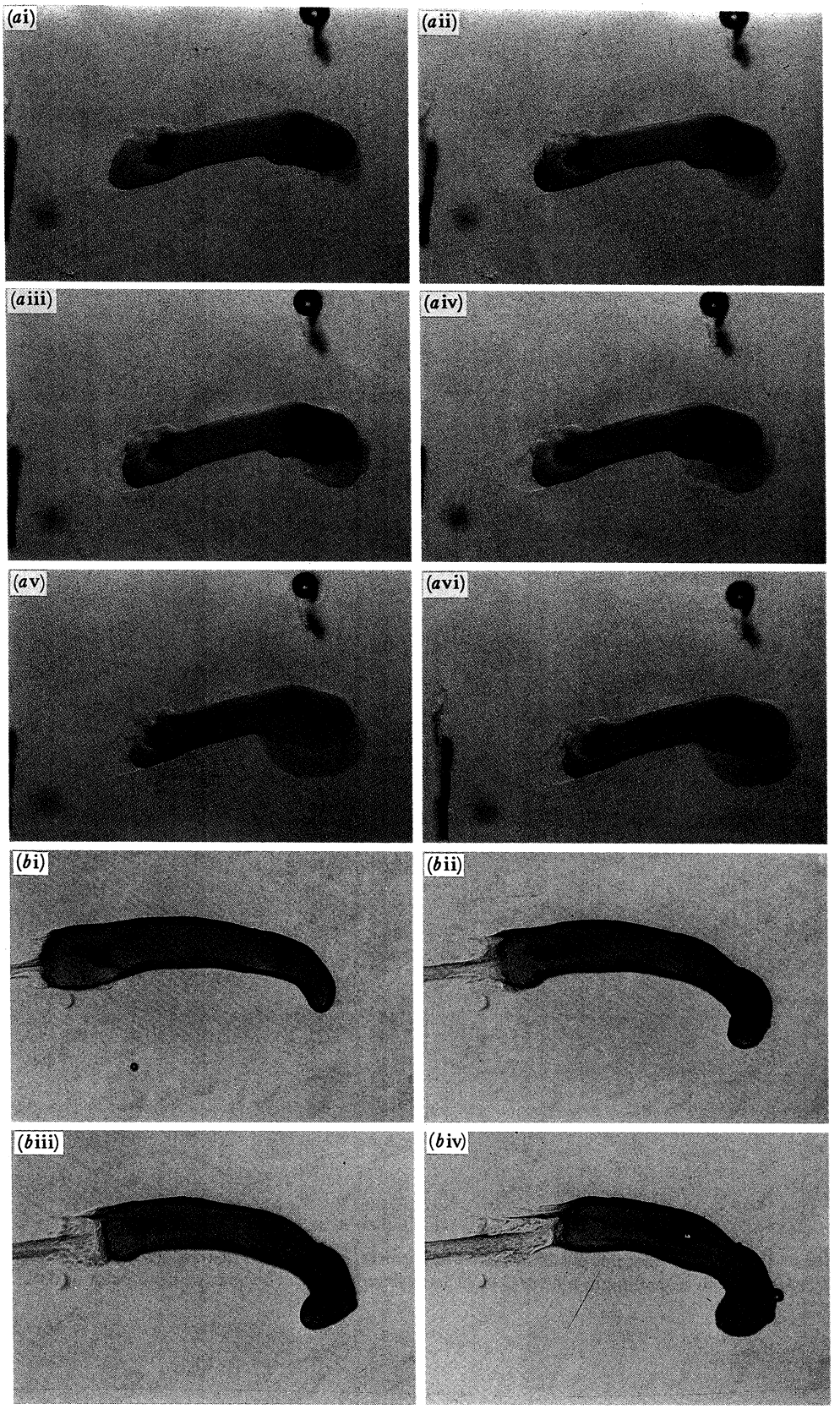

FIGURE 5. For description see opposite.

(*Facing p.* 500)

PHILOSOPHICAL TRANSACTIONS OF THE ROYAL SOCIETY B BIOLOGICAL SCIENCES

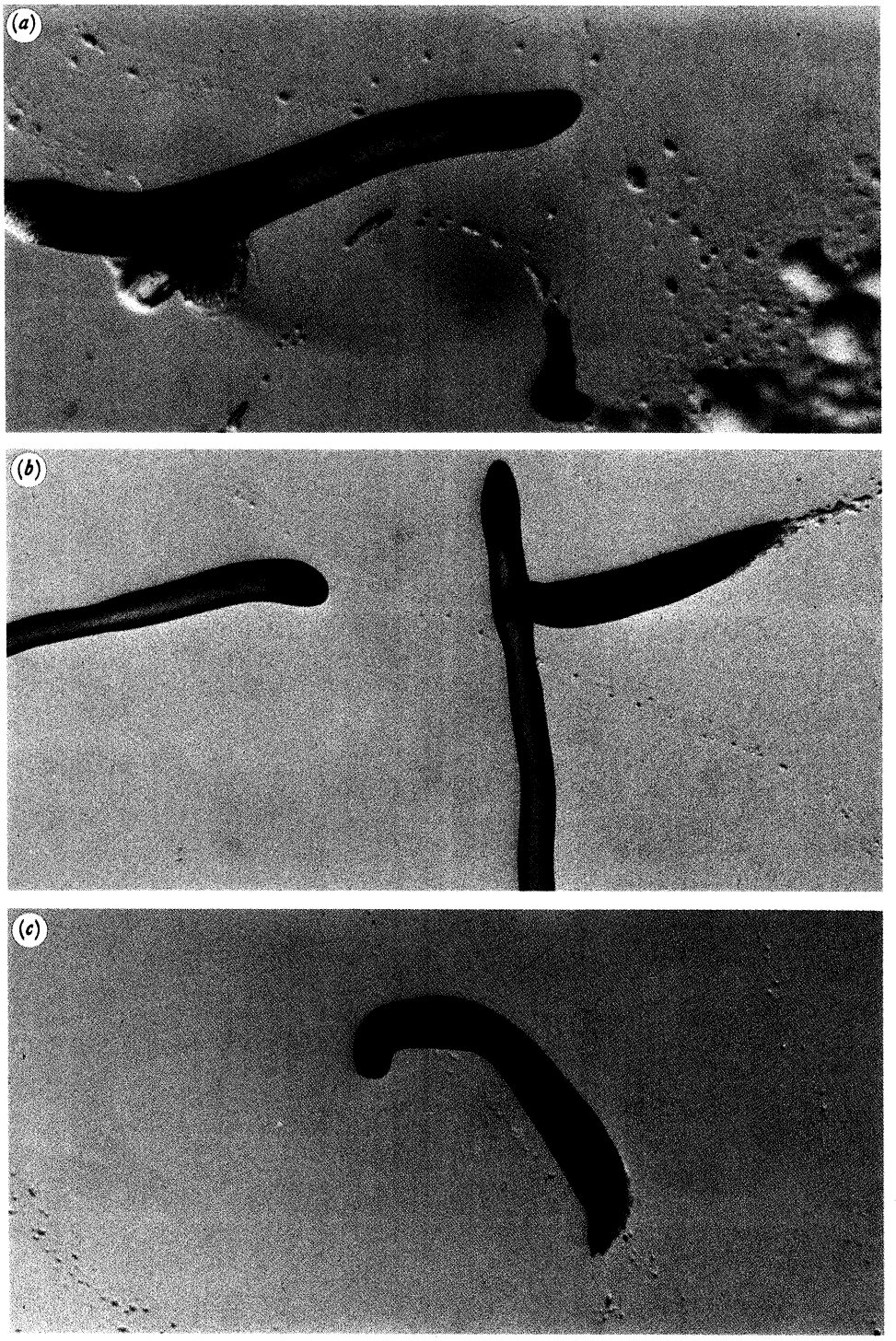

FIGURE 11. Top view photographs of free-crawling grexes, stained with neutral red dye. Note the dye concentration extending in a central river back from the tip. This persists until culmination.

PHILOSOPHICAL TRANSACTIONS OF THE ROYAL SOCIETY B BIOLOGICAL SCIENCES

Nevertheless, we reject option (i) (the boundary cells alone move the whole grex) for a variety of reasons.

(i) An observation made by Inouye & Takeuchi (1980) described at the end of §6.2.

(ii) Our own (unpublished) videotaped observation of violent circulation of cells in interior eddies in the anterior third of an imprisoned grex that we simply do not believe could be caused merely by boundary tractions.

(iii) We believe that the mechanism that makes the hemispherical aggregation mound rise vertically in air to form an elongated tower is the same mechanism that propels the grex when the tower falls over. During that vertical rise, there is no substrate for the boundary cells to crawl on. If only the cells contacting the agar floor were generating effective tractions, and they all crawled toward the central pacemakers, we would expect the aggregation mound to be shaped into a sphere (not a tower) as the boundary cells pulled the periphery in toward the centre.

(iv) Time-lapse movies of migrating grexes, made by Barbara Wang, show single slugs bifurcating axially, with the split commencing at the tip. From studying these films, we believe the axial split commences not on the agar floor but so far from the floor that the cells generating the forces to cause the split cannot gain direct traction on any solid substrate.

(v) Slugs can be observed crawling over the mycelium of a fungus (infection) in a Petri dish. Sometimes, in regions with sparse hyphae oriented more or less parallel, slugs can be seen crawling over the hyphae, perpendicular to the dominant orientation of hyphae. Then most of the length of the slug is suspended in air between the few contacts it makes with a solid substrate: a few junctions with hyphae. Nevertheless, the slug crawls, maintaining a normal shape and speed, leaving behind a normal slime sheath strung out between contact points with hyphae. It is conceivable that the events described in our fourth and fifth reasons could be caused solely by boundary amoebae interacting with a stiff slime sheath, but we regard this as unlikely.

(vi) Slugs can crawl through air from the ceiling to the floor of a Petri dish, leaving the slime sheath as a thread across the gap it crossed. Also, slugs can be put on the surface of a pool of distilled water. They migrate normally on the surface tension water–air interface, leaving their floating slime track behind. Thus, there are many instances when slug migration occurs in the absence of any solid substrate for the boundary cells to crawl upon. We therefore believe the cells in the slug must generate internally a circulatory flow, as a consequence of which the slug 'rolls' or 'swims' forward through any viscous fluid medium, for example, the slime sheath.

(vii) Referring to the caption of figure 3, we believe that the same general motive mechanism must be responsible for many apparently different morphogenetic motions in slime mould development. In particular we seek eventually to explain the symmetrically spaced radial spokes that radiate from the periodically spaced cell masses left along the culmination stalk by *Polysphondylium*. The cells generating the forces to extend those spokes (in mid air) have no solid substrate upon which to push. It seems highly unlikely that these morphogenetic deformations could be caused by mere boundary tractions.

Further reasons are discussed in §§6.2 and 6.3.

The mathematical model we now present is general. It gives a full characterization of the interaction of boundary cells with the slime sheath on agar, including their ability to crawl forward on it or slip relative to it; see §5. The chemokinetic effect of our 'second chemical' can be made nil as a trivial special case. Thus our model does not constrain us to rely entirely upon the second chemical; we can explore its effects in general, including a zero effect.

PHILOSOPHICAL TRANSACTIONS OF THE ROYAL SOCIETY B BIOLOGICAL SCIENCES

4. A mathematical model of chemotaxis in a close-packed continuum of self-propelled cells

The experiments described in the last section are preliminary. However, we believe they are sufficiently convincing, interesting, and at odds with previously published conjectures on how grexes crawl that they motivate both experimental refinements as well as a full description of the mathematical model they were designed to test. In this section and the next we present that mathematical model.

4.1. *The stress tensor should depend on the strain rate of the cell boundary velocity field*

We consider a continuum of particles with microstructure; each particle (that is, amoeba) moves about, trying to propel itself relative to the general flow of its neighbours. We imagine a closely packed swarm of such cells separated from each other by very thin layers of viscous slime which occupy a very small fraction of the volume of the swarm. We therefore disregard the slime except for the role it plays in transmitting viscous stresses between neighbouring cells.

Let the vector velocity field $\boldsymbol{v}(\boldsymbol{x}, t)$ denote the mass-averaged velocity, with respect to the 'laboratory coordinate frame', fixed in the agar plate, of the particles at position $\boldsymbol{x}$ and time t. Vector quantities are printed in bold. The expression $\boldsymbol{v}(\boldsymbol{x}, t)$ is the velocity field one would measure by plotting the trajectories of cell nucleii; it is the velocity at which the bulk cytoplasm contained in cells moves.

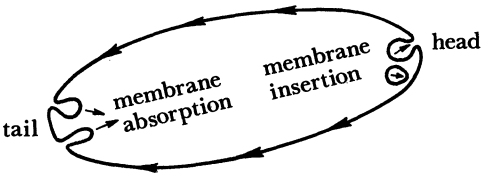

Figure 6. Schematic diagram of a cross-section of an 'Albert Harris Fountainoid' or cortical tractor model of an amoeba that can swim by generating a continuous fore to aft flow of its membrane. It does this by inserting membrane at the tip (by fusing vesicles there with its membrane), and reabsorbing membrane by pinocytosis at the rear. Note that the vesicle fusion process at the tip could serve to expel slime.

The particles have this microstructure: each has a head and a tail, and we assume each cell attempts to propel itself in the direction of its head by exerting traction upon its immediate surround. To crawl forward, this traction must be exerted from its head towards its tail. There are various ways it could exert this traction. We will assume that each cell can be modelled as an 'Albert Harris Fountainoid' (see Harris 1973) or 'cortical tractor'. This consists of an elongated cell that inserts new membrane at its head and reabsorbs membrane at its tail, thus causing a continuous membrane flow backward from head to tail. (Refer to figure 6.) This membrane flow would cause an isolated fountainoid to 'swim' through viscous fluid. The purpose of this section is to devise equations that account for how such a fountainoid would swim, not through passive viscous fluid, but through a 'fluid' consisting of closely packed copies of itself.

While the membrane fountainoid model of individual cell locomotion is easy to translate into equations, we emphasize that several different microscale models of how each cell crawls will yield the same macroscopic equations derived below.

To derive continuum differential equations characterizing our fluid of self-propelled

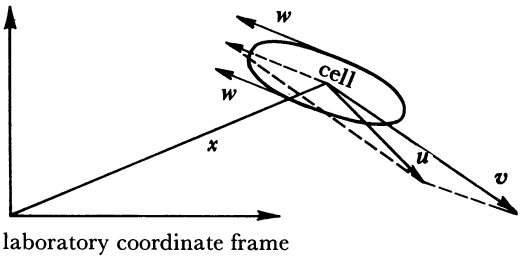

FIGURE 7. Two vector fields account for the independent mass-averaged velocity of cells with respect to the laboratory coordinate system (denoted by $\boldsymbol{v}$), and the velocity of an amoeba's membrane relative to its centre, $\boldsymbol{w}$. The vector sum of these is $\boldsymbol{u}$ and measures the velocity of the cell's membrane relative to the laboratory coordinate system.

particles, we introduce another velocity field, $\boldsymbol{w}(\boldsymbol{x}, t)$, that represents the velocity of cell membranes with respect to the geometrical centres of the cells, averaged over a small neighbourhood of cells at position $\boldsymbol{x}$ at time t. The orientations of cells near $\boldsymbol{x}$ and their membranes' speeds combine to determine $\boldsymbol{w}(\boldsymbol{x}, t)$. If cells in the vicinity of $\boldsymbol{x}$ are oriented randomly, then even though each pumps membrane backward, $\boldsymbol{w}(\boldsymbol{x}, t)$ will be almost zero. Also $\boldsymbol{w}(\boldsymbol{x}, t)$ will be zero if all cells near $\boldsymbol{x}$ have the same orientation but their membranes do not flow. When most cells near $\boldsymbol{x}$ have nearly the same aim and each generates a membrane flow, then $\boldsymbol{w}(\boldsymbol{x}, t)$ can become 'large' and represent the attempt of a small cohort of cells to crawl in the same locally preferred direction.

Let $\boldsymbol{u}(\boldsymbol{x}, t) = \boldsymbol{v}(\boldsymbol{x}, t) + \boldsymbol{w}(\boldsymbol{x}, t)$. This represents the average velocity of cell boundaries with respect to the laboratory coordinate frame at position $\boldsymbol{x}$ at time t. (Refer to figure 7.) In the next section, we will assume that the cAMP gradient at $(\boldsymbol{x}, t)$ acts to steer the direction of $\boldsymbol{w}(\boldsymbol{x}, t)$, but in this section we will ignore the mechanism that determines $\boldsymbol{w}(\boldsymbol{x}, t)$ and concentrate upon the mechanical consequences of a given $\boldsymbol{w}(\boldsymbol{x}, t)$ field.

We assume that the closely packed mass of cells is incompressible, neglecting the very slow shrinkage of each cell that presumably accompanies exudation of slime. This means:

$$\nabla \cdot \boldsymbol{v}(\boldsymbol{x}, t) = 0. \tag{4.1}$$

If no cells exert propulsive forces by moving their membranes, our continuum reduces to the classical Newtonian viscous incompressible fluid whose equations are called the Navier–Stokes equations and consist of (4.1) and:

$$\rho[(\partial \boldsymbol{v}/\partial t) + (\boldsymbol{v} \cdot \nabla)\boldsymbol{v}] = \operatorname{div} \boldsymbol{T} + \boldsymbol{b}, \tag{4.2}$$

in which $\boldsymbol{b}$ is the external body force per unit mass and $\boldsymbol{T}$ is the stress tensor for a linearly viscous fluid:

$$\boldsymbol{T} = -p\boldsymbol{I} + \mu\,[\operatorname{grad} \boldsymbol{v} + \operatorname{grad} \boldsymbol{v}^T], \tag{4.3}$$

where μ is the viscocity coefficient, ρ is the mass density, p is the hydrostatic pressure, $\boldsymbol{I}$ is the identity tensor, and

$$\boldsymbol{D} = [\operatorname{grad} \boldsymbol{v} + \operatorname{grad} \boldsymbol{v}^T] \tag{4.4}$$

is called the strain rate tensor and has components

$$\boldsymbol{D}_{IJ} = (\partial v_I/\partial x_J) + (\partial v_J/\partial x_I). \tag{4.5}$$

PHILOSOPHICAL TRANSACTIONS OF THE ROYAL SOCIETY B BIOLOGICAL SCIENCES

Equation (4.3) is a constitutive equation for stress that accounts for the fluid friction exerted by one fluid 'particle' sliding past another. We will use almost the same constitutive equation for stress; we modify it by replacing $\boldsymbol{v}$ by $\boldsymbol{u}$ in (4.3). Our active membrane tractor particles interact only at their membrane boundaries. When one such particle slides past another, the viscous shear stresses they exert upon each other through the slime lubrication layer are determined not by the relative motion of their centres, but by the relative motion of their membranes, and $\boldsymbol{u}(\boldsymbol{x}, t)$ is the velocity field that keeps track of the average membrane motion.

To generalize (4.3) correctly, replacing $\boldsymbol{v}$ by $\boldsymbol{u}$, we should allow a so-called bulk viscosity effect which accounts for viscous resistance to 'compression' of the velocity field $\boldsymbol{u}$. The bulk viscosity term was correctly omitted from (4.3) because bulk viscosity does not operate on incompressible fluids, that is, when (4.1) holds. Thus, we assert the stress tensor for our continuum of oriented closely packed membrane fountainoids to be:

$$\boldsymbol{T} = [-p + \mu_{\mathrm{B}} \operatorname{div} \boldsymbol{u}]\, \boldsymbol{I} + \mu[\operatorname{grad} \boldsymbol{u} + \operatorname{grad} \boldsymbol{u}^{T}], \tag{4.6}$$

where μ_{B} denotes a bulk viscosity coefficient. μ is the viscosity coefficient characterizing the shear stresses that arise when one amoeba moves past another. Notwithstanding the probability discussed in §3.5 that the mechanical interaction among amoebae differs from one position to another in the grex, we will take μ to be a constant. Equation (4.6) instead of (4.3) is to be substituted into the momentum balance equation, (4.2). When we do this and use (4.1) with the definition of $\boldsymbol{u}(\boldsymbol{x}, t)$ and simplify, we obtain:

$$\rho[(\partial \boldsymbol{v}/\partial t + (\boldsymbol{v} \cdot \nabla)\boldsymbol{v}] = -\operatorname{grad}[p - (\mu + \mu_{\mathrm{B}}) \operatorname{div} \boldsymbol{w}] + \mu \Delta v + \boldsymbol{b} + \mu \Delta \boldsymbol{w}, \tag{4.7}$$

where Δ represents the Laplacian operator. Thus the Ith component of $\Delta \boldsymbol{v}$ is:

$$(\Delta \boldsymbol{v})_I \equiv \sum_{j=1}^{3} \frac{\partial^2 v_I}{\partial x_J^2} \quad \text{for} \quad I = 1, 2, 3.$$

The terms $[p - (\mu + \mu_{\mathrm{B}}) \operatorname{div} \boldsymbol{w}]$ in (4.7) are, all together, no more than a complicated name for the hydrostatic pressure. It is crucial to understand the reason why to appreciate the formal argument, in the next section, that a second chemical gradient must modulate cell motion for chemotaxis to work effectively in closely packed cell swarms. In an incompressible fluid, the hydrostatic pressure field $p(\boldsymbol{x}, t)$ adjusts itself everywhere instantaneously to whatever value is necessary to satisfy the incompressibility constraint, (4.1); p just stands for whatever isotropic stress is needed to make (4.1) true. Thus, with no loss of generality we can rename the isotropic stress in (4.7) as:

$$p^* = [p - (\mu + \mu_{\mathrm{B}}) \operatorname{div} \boldsymbol{w}].$$

The same claim just made for p is true of p^* as well, so we do not distinguish between p and p^*. That is, we drop the superscript and obtain as our equations of motion for the membrane tractor continuum:

$$\rho[(\partial \boldsymbol{v}/\partial t) + (\boldsymbol{v} \cdot \nabla)\boldsymbol{v}] = -\operatorname{grad} p + \mu \Delta \boldsymbol{v} + \boldsymbol{b} + \mu \Delta \boldsymbol{w} \tag{4.8}$$

which is augmented by (4.1) to fix p.

The only difference between (4.8) and the traditional Navier–Stokes equations is the last term, which represents the effects of the active cell particles individually generating thrust by moving their membranes backwards. Thus, when $\boldsymbol{w}(\boldsymbol{x}, t) \equiv$ constant, we have exactly the Navier–Stokes equations for a dissipative, incompressible, viscous fluid, which we know to be incapable of actively generating shearing flows.

PHILOSOPHICAL TRANSACTIONS OF THE ROYAL SOCIETY B BIOLOGICAL SCIENCES

We now consider how the membrane velocity field, $\boldsymbol{w}(\boldsymbol{x}, t)$ is aimed. When $\boldsymbol{w}(\boldsymbol{x}, t)$ is determined by the gradients of *two* diffusing chemical concentration fields, (4.8) can give rise to actively sustained cell circulation flows which match those observed in the experiment described in §3. A single chemical will not work.

4.2. *Cell orientation and membrane tractor speed determined by a single chemical concentration field cannot generate cell circulation*

We want now to express mathematically the intuitive ideas presented in §2 whereby each amoeba orients itself 'in the direction of the cAMP gradient'. This is, in fact, a complicated phenomenon. The cAMP microenvironment seen by each amoeba results from a sequence of 'pulse relay' waves that sweep through the mass of cells. Schaap & Wang (1984) explain the universality of this phenomenon in cellular slime mould development. This wave propagation depends upon each cell emitting a cAMP pulse shortly after a sufficiently potent cAMP diffusion wave impinges upon it (when it is not refractory). Thus, each cell sees cAMP gradients that reverse direction as each wave passes. If cell chemotactic behaviour is similar during aggregation and in the grex, amoebae can aim to move in the direction from which a cAMP diffusion wave impinged, ignoring the direction reversal of the cAMP gradient which soon follows.

The cell sorting experiments of Sternfeld & David (1981), and of Matsukuma & Durston (1979), indicate that when a steady cAMP gradient is imposed experimentally, some cells in the grex move up that gradient. We want to formulate a mathematical model that can account both for orientation toward artificially imposed constant cAMP gradients and also for orientation in environments through which periodic cAMP diffusion wave fronts propagate. This is possible, but complicated, so complicated that it sheds no light on why a single chemical concentration field cannot organize a three-dimensional cell circulation. We therefore use, in this subsection, artificially simplistic assumptions about chemotactic steerage which will reveal the need for a second chemical concentration field. We remedy this in §4.4 by asserting a full model.

Suppose an arbitrary cAMP concentration field $c(\boldsymbol{x}, t)$ is prescribed and that each amoeba determines its orientation and the tractor speed of its membrane from that single chemical c, that is, $\boldsymbol{w}(\boldsymbol{x}, t)$ is determined by:

$$\boldsymbol{w}(\boldsymbol{x}, t) = S(c)\, \nabla c. \tag{4.9}$$

This means that $\boldsymbol{w}(\boldsymbol{x}, t) = \nabla\psi$, where

$$\psi(\boldsymbol{x}, t) = \int_0^{c(\boldsymbol{x}, t)} S(\beta)\, \mathrm{d}\beta. \tag{4.10}$$

Thus $\mu\Delta\boldsymbol{w} = \mu\nabla(\Delta\psi)$. This means the active stress term, $\mu\Delta\boldsymbol{w}$, in (4.8) can be absorbed into the hydrostatic pressure term by renaming $[p - \mu(\Delta\psi)]$ as the new hydrostatic pressure. In this way (4.8) collapses to the conventional Navier–Stokes equations for an incompressible viscous liquid, which merely dissipates the momentum of initially stirred circulation to heat. This is the mathematical demonstration of the claims made in §2.1.

PHILOSOPHICAL TRANSACTIONS OF THE ROYAL SOCIETY B BIOLOGICAL SCIENCES

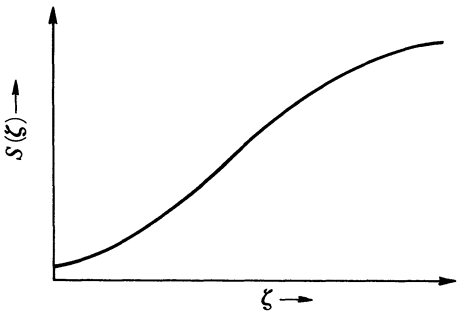

FIGURE 8. Membrane tractor speed, S, is assumed to increase as the concentration of ζ increases.

4.3. *If cell orientation is determined by* ∇c, *and membrane speed varies with* $\zeta(\boldsymbol{x}, t)$, *then unless* ∇c *and* $\nabla\zeta$ *are parallel, membrane tractors must produce active shearing flow*

Suppose that two chemical concentration fields, $\zeta(\boldsymbol{x}, t)$ and $c(\boldsymbol{x}, t)$ are prescribed arbitrarily, and that each cell's membrane tractor velocity, with respect to its geometrical centre, is determined by:

$$\boldsymbol{w}(\boldsymbol{x}, t) = -S(\zeta)\,\nabla c, \tag{4.11}$$

where $S(\zeta)$ is an increasing function of ζ as shown in figure 8. That is, cell orientation is parallel to ∇c and membrane speed is $S(\zeta)$ opposite to that aim.

Equation (4.11) models an attempt by individual amoebae to move up the cAMP gradient, and can therefore properly be called a three-dimensional chemotaxis model. From (4.11) we have

$$\mu\Delta\boldsymbol{w} = -\mu\nabla[\Delta(S(\zeta)\,c)] - \mu\Delta[cS'(\zeta)\,\nabla\zeta], \tag{4.12}$$

where $S'(\zeta) = \mathrm{d}S/\mathrm{d}\zeta$.

The first term in (4.12) is ineffectual because it gets absorbed into the hydrostatic pressure field when (4.12) is substituted into (4.8). After renaming the hydrostatic pressure once again, (4.12) substituted into (4.8) yields:

$$\rho[(\partial\boldsymbol{v}/\partial t) + (\boldsymbol{v}\cdot\nabla)\boldsymbol{v}] = -\operatorname{grad} p + \mu\Delta\boldsymbol{v} + \boldsymbol{b} - \mu\Delta[cS'(\zeta)\,\nabla\zeta].$$

The last term in this equation cannot be counteracted by any hydrostatic pressure field unless $\nabla\zeta$ and ∇c happen to be parallel. This means imposed non-parallel gradients of ζ and c will cause an active shear flow of cell tractors.

Finlayson & Scriven (1969) obtained essentially the same active stress constitutive equation as we will use by a different route. They posed the following abstract questions: is it possible to construct a frame-indifferent constitutive equation for a stress tensor from the gradients of chemical concentration fields that leads to spontaneous active generation of shearing flows? If so, what is the minimum number of chemical gradients needed and what is the form of the constitutive equation? Finlayson & Scriven (1969) found the minimum number of chemicals needed was two (as we have), and they showed that, when only first gradients of those two fields were allowed in the formula for stress, there were only two distinct kinds of 'chemically steered' active stress tensors. They called one of these the 'symmetric deviatoric stress' and the formula for it closely resembles the one we have just derived.

From a purely mathematical point of view we could concoct the second required chemical field as $\zeta = \|\nabla c\|$. Our analysis shows this choice capable of generating active shear flows, but unrealistic ones. It is also a biologically silly choice so we have rejected it.

When (4.11) is substituted into (4.6), and the isotropic part of the resulting stress is renamed as just p, we obtain:

$$\boldsymbol{T}_{IJ} = -p\delta_{IJ} + \mu[(\partial v_I/\partial x_J) + (\partial v_J/\partial x_I)] - \mu S'(\zeta)\{[(\partial c/\partial x_I)(\partial\zeta/\partial x_J)] + [(\partial c/\partial x_J)(\partial\zeta/\partial x_I)]\} - 2\mu S(\zeta)(\partial_2 c/\partial x_J \partial x_I). \quad (4.13)$$

On the right-hand side of (4.13), the first two terms are the conventional dissipative Newtonian stress tensor. The last term was excluded from consideration by Finlayson & Scriven (1969) on aesthetic grounds. The terms in (4.13) contained in curly brackets (minus one third of its trace) is precisely Finlayson & Scriven's symmetric deviatoric stress, multiplied by a coefficient modulated by the concentration, ζ. Finlayson & Scriven's formal continuum mechanics approach, and our attempt to deduce a stress tensor from assumed microscale behaviour of the participating particles, both converge to equivalent results. This congruence fortifies the validity of both approaches.

4.4. *A differential equation, not an algebraic one, should determine cell orientation*

In the preceding subsection, we considered a much oversimplified determination of $\boldsymbol{w}(\boldsymbol{x}, t)$ to make the point that at least two chemical concentration fields are needed to generate an effective active shear flow. Equation (4.11) oversimplifies because it asserts that, when amoebae experience changed local chemistry, either beause they move or because the chemistry varies by reaction and diffusion, they re-orient *instantly*. In fact such adjustment to new chemical cues must occur gradually, so we must use a more complex mathematical model for cell orientation. Under certain circumstances, this new formulation will reduce to (4.11).

We factor $\boldsymbol{w}(\boldsymbol{x}, t)$ into a membrane flow speed, $S(\zeta)$, and a vector field, $\boldsymbol{e}(\boldsymbol{x}, t)$, that keeps track of the average orientation of amoebae at $\boldsymbol{x}$ at time t. Thus we have:

$$\boldsymbol{w}(\boldsymbol{x}, t) = -S(\zeta)\,\boldsymbol{e}(\boldsymbol{x}, t). \quad (4.14)$$

The expression $\|\boldsymbol{e}\|$ denotes the norm or length of $\boldsymbol{e}$. When $\|\boldsymbol{e}(\boldsymbol{x}, t)\| = 0$, this does not mean that no amoeba is oriented, but that the amoebae near $\boldsymbol{x}$ are oriented randomly. $\|\boldsymbol{e}(\boldsymbol{x}, t)\| = 1$ means every amoeba at $\boldsymbol{x}$ is oriented in exactly the same direction. This can never happen, so our formulation must preclude $\|\boldsymbol{e}(\boldsymbol{x}, t)\| \geqslant 1$.

Before we discuss the way $\boldsymbol{e}(\boldsymbol{e}, t)$ rotates in response to chemical cues, we must model the cAMP signalling process discussed in §4.2. The idea is to model the following behaviour of each amoeba:

(i) each cell emits a cAMP pulse shortly after a cAMP diffusion wave impinges upon it, but see (iii);

(ii) the same diffusion wave that triggers (i) also induces a cell to orient itself toward the direction from which that wave arrived;

(iii) after echoing a pulse as in (i), a cell is refractory to further cAMP stimulation of both pulse echoing and re-orientation for a while.

Goldbeter & Segel (1977) proposed a mathematical model for items (i) and (iii), to which we will append a characterization of (ii). Their model is thoroughly described by Segel (1984). It involves three chemicals: two within a cell, and cAMP ejected from the cell into extracellular space. As shown by Segel, that model can be simplified so that only two chemicals need be considered: α = ATP (segregated within certain membrane compartments inside the cell),

PHILOSOPHICAL TRANSACTIONS OF THE ROYAL SOCIETY B BIOLOGICAL SCIENCES

and c = external cAMP. Goldbeter & Segel considered a well-stirred situation and devised equations of the form:

$$dc/dt = f(\alpha, c) \equiv \pi\Phi(\alpha, c) - kc, \tag{4.15}$$

$$d\alpha/dt = g(\alpha, c) \equiv \Gamma - \sigma\Phi(\alpha, c), \tag{4.16}$$

where

$$\Phi(\alpha, c) \equiv \frac{\alpha^2(1+c)^2}{L+\alpha^2(1+c)^2}, \tag{4.17}$$

and π, k, Γ, σ, and L are parameters.

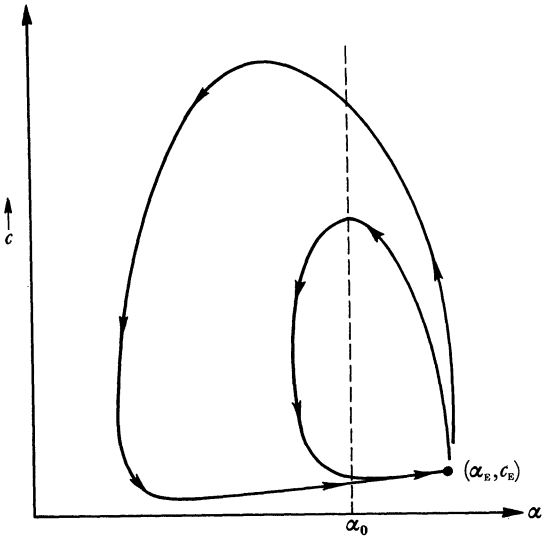

FIGURE 9. Phase portrait for the ODE system (4.15)–(4.17) when parameters are tuned to give relay (but not autonomous oscillatory) behaviour. There is a unique stable equilibrium point, (α_E, c_E). If c is increased slightly above c_E (by arrival of a cAMP diffusion front), then the phase trajectory involves a large excursion through phase space before return to the equilibrium point. c increases rapidly as α falls, and this represents the amplified echo of the received cAMP pulse. Then c falls while α gradually recovers its equilibrium value. During this recovery, the cell governed by (4.15)–(4.17) is relatively refractory to further cAMP stimulation.

These are equations (15*a*), (15*b*), and (16) in chapter 6 of Segel (1984). The details are not important here, but the qualitative behaviour of these equations is important. Certain parameter values in these equations cause autonomous oscillatory behaviour, corresponding to periodic pulse emissions of cAMP, which we will assume cells in the grex tip exhibit. Slightly different parameter values preclude spontaneous oscillation but cause cAMP pulse echo behaviour. That is, for the echo behaviour parameter setting, the phase portrait for the ODE system (4.15) and (4.16) is as shown in figure 9, and this is the cAMP signalling behaviour we will assume most of the cells in the grex follow.

We assume the chemical α remains within cells and does not diffuse, so the following equation accounts for the reaction and convection of α throughout the grex:

$$\partial\alpha/\partial t = -\boldsymbol{v}\cdot\nabla\alpha + g(\alpha, c). \tag{4.18}$$

c (cAMP) diffuses through the slime between the cells and is convected at the velocity of the cell membranes relative to the lab frame, so the conservation equation for c is:

$$\partial c/\partial t = -\nabla\cdot(c\boldsymbol{u}) + \nabla\cdot(D_c\nabla c) + f(\alpha, c). \tag{4.19}$$

PHILOSOPHICAL TRANSACTIONS OF THE ROYAL SOCIETY B BIOLOGICAL SCIENCES

To account for the observation that amoebae orient toward impinging cAMP waves, but are then relatively refractory to re-orientation for a while so that they do not reverse orientation when they see the reverse gradient as the cAMP diffusion wave passes, we will assume that amoebae re-orient 'rapidly' when α is high, and slowly when α is low. We do this formally by asserting the following conservation equation for e:

$$(\partial \boldsymbol{e}/\partial t) + (\boldsymbol{v}\cdot\nabla)\,\boldsymbol{e} = \Omega\Delta\boldsymbol{e} - \nu\boldsymbol{e} + (1-\|\boldsymbol{e}\|)\,\eta(\alpha)\,\nabla c \tag{4.20}$$

in which $\eta(\alpha)$ is shown in figure 10. The left-hand side of (4.18) is the rate of change of the orientation field, $\boldsymbol{e}(\boldsymbol{x}, t)$, as seen riding along at the mass averaged velocity (that is, riding with an amoeba). On the right-hand side, the first term is one that acts to smooth the $\boldsymbol{e}$ field globally. In practice, however, we will assume $\Omega = 0$. The last term says that $\boldsymbol{e}(\boldsymbol{x}, t)$ rotates toward ∇c provided α is 'high' near $\boldsymbol{x}$ (refer to figure 10). The factor $(1-\|\boldsymbol{e}\|)$ in this last term prevents $\boldsymbol{e}(\boldsymbol{x}, t)$ from ever attaining perfect alignment. If the orientation of cells is not continually reinforced, the $-\nu\boldsymbol{e}$ term in (4.20) attenuates cell alignment and leads eventually to random cell orientation in the absence of cAMP gradients.

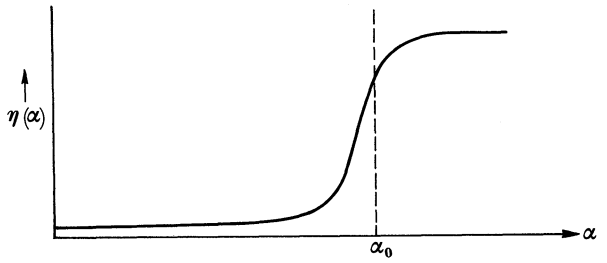

FIGURE 10. The rate at which the cell orientation rotates to track the cAMP gradient is $\eta(\alpha)$. For high α, that is when the cell is ready to be triggered or has just been triggered, η is large so the cell can quickly re-orient. When α is low, that is while the cell is refractory to cAMP stimulation, η is small to slow down the re-orientation process.

In cases where cells experience constant c and α concentration fields, and $\Omega = 0$, then (4.20) reduces to:

$$\boldsymbol{e} = (1-\|\boldsymbol{e}\|)\,\frac{\eta(\alpha)}{\nu}\,\nabla c,$$

which can be solved to yield:

$$\boldsymbol{e} = \frac{\nabla c}{\eta(\alpha)/\nu + \|\nabla c\|}. \tag{4.21}$$

Equations (4.21) and (4.14) are equivalent to (4.11), so that the considerations of §§4.2 and 4.3 still provide valid insight into the expected behaviour of our model, even when (4.20) and (4.14) determine the membrane velocity field, $\boldsymbol{w}$.

Finally we need a conservation equation for the chemical ζ whose concentration modulates the membrane tractor speed. We assume ζ to be a metabolite, produced by all cells, and we assume it moves both by diffusion and convection in the slime. Thus, we have

$$\partial\zeta/\partial t = \nabla\cdot(D_\zeta\nabla\zeta) - \nabla\cdot(\boldsymbol{u}\zeta) + \Sigma, \tag{4.22}$$

where Σ is the rate ζ is produced by each cell.

Because higher ζ leads to higher membrane traction by cells, which will create a local

churning of the slime lubrication layers, we expect both D_c and D_ζ to increase as ζ increases. We return to this issue in §5.1. Note here that we have written equations (4.19) and (4.22) to allow arbitrary variations of these two diffusivity coefficients.

By solving (4.18) and (4.19) numerically (with $\boldsymbol{v} = 0$ and $\boldsymbol{u} = 0$), we have verified that cAMP waves initiated in a small region of cells capable of autonomous oscillation propagate through an adjacent large domain of relay-competent cells (incapable alone of autonomous oscillation).

5. Simplification of the general model to account for a grex trapped in a long tube

5.1. *The model reduces to an initial, boundary value problem for two scalar parabolic* PDEs *in one space dimension*

In this section we assert the boundary constraints on, and simplifications of, our general model appropriate to obtain its simplest possible instance capable of being compared to actual experiments. This simplification process leads to the solutions discussed in §2 and shown in figure 2. The full model, while computationally complicated and expensive to solve on a computer, is, we believe, tractable. Work to solve it without making the following restrictive simplifications is in progress and will be presented in a future publication.

To avoid the mathematical complexity of cylindrical polar coordinates, we consider not a circular cylindrical tube, but a region between flat, rigid, horizontal plates. Nothing varies along the axis perpendicular to the plane of the drawing. Referring to figure 2, the y-axis points perpendicular to the plates, and the x-axis lies along the midline between the plates. In the following discussion, 'axial' refers to displacement along the x-axis, and 'radial' refers to displacement along the y-axis away from $y = 0$. The plates are located at $y = -h$ and $y = +h$, so $|y| = h$ is the analogue of the boundary of the grex. We assume symmetry of the solution across the $y = 0$ midline.

While we believe axial propagation of pulses of cAMP orients the cells, we consider a much simpler situation here: cell orientation caused by an imposed linear axial cAMP gradient. We attempt a model of a very long grex having a steady cAMP source 'far to the right' toward $x = +\infty$ and having, toward $x = -\infty$, a cAMP sink. This means we neglect the chemical kinetics that produce and degrade cAMP, so we can totally ignore (4.18) and set $f(\alpha, c) = 0$ in (4.19). We account only for the transport of c by diffusion and convection.

The most severe simplification we make is to ignore the curved cell trajectories that must exist at the tip, near the presumed cAMP source, and at the tail of an imprisoned grex. We speculate that these curved cell trajectories should look as shown in figure 4, but we emphasize that we have not yet actually computed them. We intend our simplifed model to apply to the mid section of the grex, excluding both tip and tail. In this section, only the hydrostatic pressure and the cAMP field vary with the axial coordinate, x. By symmetry, cells in this mid section must move parallel to the confining plates, although they need not be aimed axially. According to the solutions of the equations we derive in this section, cells turn out to aim and try to crawl inward toward the midline but are driven axially by the resultant effects of their crawling neighbours.

Let g denote the imposed axial cAMP gradient. Below, bold type denotes 2-vector quantities while subscripted quantities are their cartesian components. The expression $\boldsymbol{x} = (x_1, x_2) = (x, y)$

means y is another name for the second component of $\boldsymbol{x}$. The simplifying assumptions we have just made are rendered mathematically as follows:

$$\boldsymbol{V}(\boldsymbol{x}, t) = (V_1(y, t), 0) \tag{5.1}$$

$$\boldsymbol{w}(\boldsymbol{x}, t) = (w_1(y, t), w_2(y, t)) \tag{5.2}$$

$$\zeta(\boldsymbol{x}, t) = \zeta(y, t) \tag{5.3}$$

$$c(\boldsymbol{x}, t) = C(y, t) + gx. \tag{5.4}$$

$C(y, t)$ is the perturbation caused by convection and diffusion from the imposed uniform axial gradient ($c = gx$) of cAMP.

When we neglect the body force (for example, gravitational acceleration), $\boldsymbol{b}$, (5.1) and (5.2) reduce the momentum balance equation (4.8) to these two component equations:

$$\rho(\partial V_1/\partial t) = -(\partial p/\partial x) + \mu(\partial^2/\partial y^2)\ (V_1 + w_1) \tag{5.5}$$

$$0 = -(\partial p/\partial y) + 2\mu(\partial^2 w_2/\partial y^2). \tag{5.6}$$

By differentiating both (5.5) and (5.6) with respect to x, we can prove that the pressure field must have this form:

$$p(x, t) = P(y, t) + G(t)\ x, \tag{5.7}$$

where $G(t)$ is the axial pressure gradient. To model the special circumstances of a grex trapped in a plugged tube, we will compute the value of $G(t)$ needed to preclude net axial movement of the imprisoned grex. Because grexes are so small and move so slowly, that is, the Reynolds number is vanishingly small, inertial effects are completely negligible. We can therefore neglect the left-hand side of (5.5), so that with (5.7), (5.5) becomes:

$$(\partial^2/\partial y^2)\ (V_1 + w_1) = G(t)/\mu. \tag{5.8}$$

Simplified as described above, (4.19) becomes:

$$\partial C/\partial t = -g(V_1 + w_1) + (\partial/\partial y)\ [D_c(\partial C/\partial y)] - [C(y, t) + gx]\ (\partial w_2/\partial y). \tag{5.9}$$

An inconsistency is apparent: the $gx(\partial w_2/\partial y)$ term in (5.9) leads to variations of *everything* with respect to x, contradicting (5.1)–(5.4). Owing to an imposed linear increase of c with x, the radial convection this term represents has a greater effect to the right of the domain, toward increasing x, than to the left. To circumvent this difficulty we will ignore radial convection, based on the assumption that w_2 and its gradients will be small compared to V_1 and w_1. This assumption can be verified after we have computed a solution. With this approximation, (5.9) becomes:

$$\partial C/\partial t = -g(V_1 + w_1) + (\partial/\partial y)\ [D_c\,(\partial C/\partial y)]. \tag{5.10}$$

Equation (4.21) becomes:

$$\partial\zeta/\partial t = (\partial/\partial y)\ [D_\zeta\,(\partial\zeta/\partial y)] + \Sigma. \tag{5.11}$$

Symmetry across the $y = 0$ midline implies these boundary conditions:

$$(\partial C/\partial y) = 0 \quad \text{and} \quad (\partial\zeta/\partial y) = 0 \quad \text{at} \quad y = 0, \tag{5.12}$$

$$\partial V_1/\partial y = 0 \quad \text{at} \quad y = 0. \tag{5.13}$$

We assume cAMP does not leak out of the grex at its boundary which means:

$$\partial C/\partial y = 0 \quad \text{at} \quad y = h. \tag{5.14}$$

PHILOSOPHICAL TRANSACTIONS OF THE ROYAL SOCIETY B BIOLOGICAL SCIENCES

We assume that ζ evaporates at the grex surface so that its concentration is zero there:

$$\zeta(h, t) = 0. \tag{5.15}$$

We will use the quasi-steady version of (4.20), namely (4.21) in which we give the name ψ to $\eta(\alpha)/\nu$. Remember we are ignoring the equation for α altogether so that α must be constant. Thus we have this simplified orientation field:

$$\boldsymbol{e} = (e_1, e_2) = [1/(\psi + \|\nabla c\|)]\ [(\partial c/\partial x), (\partial c/\partial y)].$$

From (5.4) and (4.14) this yields:

$$w_1 = -\frac{S(\zeta)\ g}{\psi + [g^2 + (\partial C/\partial y)^2]^{\frac{1}{2}}}$$

and

$$w_2 = -\frac{S(\zeta)\ (\partial C/\partial y)}{\psi + [g^2 + (\partial C/\partial y)^2]^{\frac{1}{2}}}. \tag{5.16}$$

We can integrate (5.8) twice with respect to y and use (5.13) to set one of the integration 'constants' to zero to obtain:

$$V_1 + w_1 = G(t)\ y^2/2\mu + B(t). \tag{5.17}$$

We now derive a condition that allows cells to slide at the junction between amoebae and the rigid boundary of the prison. Strictly speaking, a viscous fluid, even one that generates active stress, should adhere to any fixed rigid boundary it touches. We want, however, to account for the fact that a relatively thick slime sheath separates the amoebae from the rigid substratum. Conceivably the cells can slip parallel to the substratum lubricated by the slime. We allow this by assuming that the component of stress tangent to the wall at $|y| = h$ (the left-hand side of (5.18)) is proportional to the slip velocity of the cells' membranes, $\boldsymbol{u}$, relative to that wall (the right-hand side of (5.18)). δ is the proportionality constant; Q is the net forward speed of the grex down the tube, yet to be determined.

$$-\mu[(\partial V_1/\partial y) + (\partial w_1/\partial y)]\,|_{y=h} = \delta(V_1 + w_1 + Q)\,|_{y=h}. \tag{5.18}$$

When we combine (5.17) with (5.18) we obtain:

$$-\mu\ (G(t)h/\mu) = \delta\,[G(t)\ h^2/2\mu) + B(t) + Q]. \tag{5.19}$$

The axial pressure gradient, multiplied by the length and cross-sectional area of a grex, is the force available to roll out the slime sheath. We expect this force to be roughly proportional to the rate at which the viscous sheath is rolled out. Thus the net forward speed should be proportional to the axial pressure gradient. Here we assume that

$$Q = rG,$$

where r is a constant depending on grex geometry and slime rheology. Then we can solve (5.19) for $B(t)$ in terms of $G(t)$:

$$B(t) = -\left[r - \frac{h}{\delta}\left(1 + \frac{h\delta}{2\mu}\right)\right] G(t). \tag{5.20}$$

Combining (5.20) with (5.17) yields:

$$V_1(y, t) + w_1(y, t) = G(t)\left[\frac{y^2}{2\mu} - r - \frac{h}{\delta}\left(1 + \frac{h\delta}{2\mu}\right)\right]. \tag{5.21}$$

This, with (5.16), gives an algebraic equation determining the axial mass-averaged velocity profile in terms of the fields $\zeta(y, t)$ and $C(y, t)$.

$$V_1(y, t) = \frac{gS(\zeta)}{\psi + [g^2 + (\partial C/\partial y)^2]^{\frac{1}{2}}} + G(t)\left[\frac{y^2}{2\mu} - r - \frac{h}{\delta}\left(1 + \frac{h\delta}{2\mu}\right)\right]. \tag{5.22}$$

This is the answer we want to compute, and is the solution graphed in figure 2. It predicts the axial velocity cell nuclei should move in the imprisoned grex as a function of distance from its axis. We now determine $G(t)$, which is the pressure gradient required to push the grex down the tube at speed $Q = rG$. When the grex is in a dead-end prison, Q must be zero, so $r = 0$ corresponds to the simulation of an imprisoned grex shown in figure 2*a*. In §2.6 we discussed the interpretation of this pressure gradient further in the $(r = 0)$ fully stalled case. $G(t)$ is determind by substituting (5.22) into the constraint:

$$\int_0^h V_1(y, t)\, \mathrm{d}y = Qh = rhG,$$

and this can be solved explicitly for $G(t)$ to yield:

$$G(t) = \frac{1}{2rh + h^2\,(h/3\mu + 1/\delta)} \int_0^h \frac{gS(\zeta)}{\psi + [g^2 + (\partial C/\partial y)^2]^{\frac{1}{2}}}\, \mathrm{d}y. \tag{5.23}$$

Equation (5.23) substituted back into (5.22) gives an explicit recipe for the velocity profile we seek in terms of the fields $C(y, t)$ and $\zeta(y, t)$. These fields are determined by the partial differential equations (5.10) and (5.11). To these we add one final detail. A submicroscopic movie of individual cells crawling over each other would probably show 'churning' of the slime lubrication layer with an intensity that increases as the function $S(\zeta)$ (from equation (4.14)) increases. In this way, higher concentrations of ζ should lead to higher local diffusivities of both c and ζ, especially if there is some randomness in the local orientation of cells. To account for this chemokinetic augmentation of diffusive transport, we let D_c and D_ζ depend upon ζ as follows:

$$D_c = D_c^0[1 + \epsilon^* S(\zeta)]; \quad D_\zeta = D_\zeta^0[1 + \epsilon^* S(\zeta)]. \tag{5.24}$$

When we substitute (5.24) and (5.21) into (5.10) and (5.11) we obtain the PDE initial, boundary value problem needing numerical solution before (5.22) with (5.23) can determine the mass-averaged velocity profile we seek. It comprises the following two equations:

$$\partial C/\partial t = -gG(t)\left[\frac{y^2}{2\mu} - r - \frac{h}{\delta}\left(1 + \frac{h\delta}{2\mu}\right)\right] + \frac{\partial}{\partial y}\left\{D_c^0[1 + \epsilon^* S(\zeta)]\,\frac{\partial C}{\partial y}\right\} \tag{5.25}$$

$$\partial\zeta/\partial t = (\partial/\partial y)\,\{D_\zeta^0[1 + \epsilon^* S(\zeta)]\,\partial\zeta/\partial y\} + \Sigma. \tag{5.26}$$

$G(t)$ is given in (5.23). Boundary conditions for (5.25) and (5.26) are given as equations (5.12), (5.14), and (5.15). For initial conditions, we use $C(y, 0) = 0$ and $\zeta(y, 0) = 0$.

Even though the functional form for $S(\zeta)$ makes little difference in the behaviour of our model, to complete the specification of the computer calculation we did, we must choose *some* definite functional form. The next equation does this:

$$S(\zeta) = S_0\,\frac{q^* + \zeta}{\theta^* + \zeta} \tag{5.27}$$

PHILOSOPHICAL TRANSACTIONS OF THE ROYAL SOCIETY B BIOLOGICAL SCIENCES

where S_0 is the maximum speed that one amoeba can crawl as ζ becomes very high. When $\zeta = 0$, cells crawl at the speed $(q^*/\theta^*)\,S_0$. The graph of (5.27) is as shown in figure 8. Only the qualitative shape of this graph is important, not the explicit recipe in (5.27).

At this stage, our model involves 13 parameters:

$$S_0,\ q^*,\ \theta^*,\ g,\ \mu,\ h,\ \delta,\ \epsilon^*,\ D_c^0,\ D_\zeta^0,\ \Sigma,\ r, \text{ and } \psi.$$

In the next subsection, we introduce dimensionless variables and reduce the parameter count.

5.2. *Introducing dimensionless variables reduces the parameter count*

We now give new dimensionless names to the original variables in our simplified model derived in the preceding subsection. No further simplifications, approximations, or new assumptions are involved. Instead, the point here is to collapse the set of 13 parameters into a completely equivalent set of eight dimensionless ratios. The important intuitive meaning of this equivalence is that five of the original parameters are redundant: variation of one can be completely offset by variations in others. It is better to expose this redundancy explicitly rather than discover it accidentally through costly computer simulations. We will not discuss the details of this process but simply assert the results and the rules needed to transform from the dimensionless variables used below back to the original dimensioned variables in the previous subsection.

Define the following eight dimensionless parameters:

$$S \equiv \frac{\mu}{h\delta},\quad \phi \equiv \frac{\psi}{g},\quad d \equiv \frac{D_c^0}{D_\zeta^0},\quad J \equiv \frac{hS_0}{D_\zeta^0}$$

$$q \equiv \frac{q^*h^2\Sigma}{D_\zeta^0},\quad \theta\frac{\theta^*h^2\Sigma}{D_\zeta^0},\quad \epsilon = \epsilon^*S_0,\quad R = \frac{2\mu r}{h^2}. \tag{5.28}$$

Let

$$A(\Upsilon) \equiv (q+\Upsilon)/(\theta+\Upsilon). \tag{5.29}$$

Let

$$\Lambda(z,\tau) \equiv \frac{A(\Upsilon)}{\phi + [1+(\partial\mathscr{H}/\partial z)^2)^{\frac{1}{2}}}. \tag{5.30}$$

Let

$$\Theta(\tau) \equiv \int_0^1 \Lambda(z,\tau)\ \mathrm{d}z. \tag{5.31}$$

Solve the following initial, boundary value problem:

$$\frac{\partial\Upsilon}{\partial\tau} = \frac{\partial}{\partial z}\left([1+\epsilon A(\Upsilon)]\frac{\partial\Upsilon}{\partial z}\right)+1, \tag{5.32}$$

$$\frac{\partial\mathscr{H}}{\partial\tau} = -J\Theta(\tau)\,\frac{z^2-1-2s-2R}{2(s+1/3+R)}+\mathrm{d}\,\frac{\partial}{\partial z}\left([1+\epsilon A(\Upsilon)]\frac{\partial\mathscr{H}}{\partial z}\right) \tag{5.33}$$

with boundary, initial conditions:

$$\partial\Upsilon/\partial z = \partial\mathscr{H}/\partial z = 0 \quad \text{at} \quad z = 0,\quad \partial\mathscr{H}/\partial z = 0,\quad \Upsilon = 0 \quad \text{at} \quad z = 1,$$
$$\text{and} \quad \Upsilon(z,0) = \mathscr{H}(z,0) = 0. \tag{5.34}$$

PHILOSOPHICAL TRANSACTIONS OF THE ROYAL SOCIETY B BIOLOGICAL SCIENCES

When that is done, the solution of the problem in terms of the original variables is recovered by the following conversion formulae:

$$t \equiv (h^2/D_\zeta^0)\,\tau, \quad y \equiv hz, \tag{5.35}$$

$$\zeta(y,t) \equiv \frac{\Sigma h^2}{D_\zeta^0}\,\Upsilon(z,\tau), \quad C(y,t) \equiv hg\mathscr{H}(z,\tau)$$

$$V_1(y,t) \equiv S_0\left\{\Lambda(z,\tau) + \frac{\Theta(\tau)\,(z^2-1-2s-2R)}{2(s+1/3+R)}\right\} \tag{5.36}$$

$$w_1 = \frac{-S_0\,gA(\Lambda)}{\phi + [1+(\partial\mathscr{H}/\partial z)^2]^{\frac{1}{2}}} \tag{5.37}$$

$$w_2 = \frac{-S_0\,gA(\Lambda)\,\partial\mathscr{H}/\partial z}{\phi + [1+(\partial\mathscr{H}/\partial z)^2]^{\frac{1}{2}}} \tag{5.38}$$

$$Q = \frac{S_0\,R\Theta(\tau)}{2(R+S+1/3)}. \tag{5.39}$$

Finally, the angle made by the cell orientation vector field, $\boldsymbol{e}$, with the x-axis is

$$\tan^{-1}(\partial \mathrm{H}/\partial z). \tag{5.40}$$

We solved the PDE initial, boundary value problem stated above in equations (5.32), (5.33), and (5.34) numerically by using the method of lines with second order centred difference approximations of spatial gradients. The resulting system of ordinary differential equations was solved with a variable order (up to sixth) implicit Adams–Moulton multistep algorithm that controls the step size automatically to keep the local discretization error within a specified tolerance. It is not an expensive calculation.

For the parameter values we tried, solutions to (5.33) and (5.34) approached a steady-state equilibrium as τ increased from 0 to about 2 and thus $\zeta(y,t)$, ∇c, $V_1(y,t)$, $w_1(y,t)$, and $w_2(y,t)$ attained steady-state equilibrium. Even though ∇c reaches steady-state, $c(x,y,t)$ never does. This is because the w_1 contribution to cAMP convection carries cAMP from right to left more potently to the right of the domain than to the left. Integrate (5.33) from $z=0$ to $z=1$ to see that the integral of $\mathscr{H}$ will be an ever-increasing function of τ. This is an artefact of assuming an imposed linear axial cAMP gradient instead of propagating fronts of cAMP relay pulses. In our solutions, as $\tau\to\infty$, $\mathscr{H}(z,\tau)$ becomes the superposition of a steady-state function of z with a linearly increasing function of τ. Note that only the gradient of c is important in determining the $\boldsymbol{e}$ orientation field, so the ever-increasing c concentration has no effect mechanically in our model.

A typical solution for an imprisoned slug ($R=0$, so $Q=0$) is shown in figure 2*a*. The values of the eight dimensionless parameters used were: $s=0.01$, $\phi=0.5$, $d=1$, $J=0.5$, $q=0.045$, $\theta\equiv 0.15$, and $\epsilon\equiv 0.5$, and $R=0$, $\frac{1}{4}$, $\frac{3}{4}$, and 2 in figure 2*a*, *b*, *c*, and *d*, respectively. Larger values of R signify lower resistance to net forward movement.

PHILOSOPHICAL TRANSACTIONS OF THE ROYAL SOCIETY B BIOLOGICAL SCIENCES

6. The model and the literature

Here we shall review the extensive literature on slug movement to assess which experimentally known facts support the model presented above, and which seem inconsistent with it, at least with its simplest case. For conceptual simplicity, we adopted in our introduction the hypothesis that all grex cells are identical except the tip pacemakers. In this section, we will find that this hypothesis probably needs to be modified. We discuss here: cell differentiation; movement of cells grafted into a grex; chemotaxis and orientation of individual cells within the slug; and chemotaxis of the whole slug. In addition, we speculate about the identity of the second chemokinesis chemical whose existence we were forced to postulate on abstract grounds.

6.1. *Cell differentiation*

In some species of cellular slime moulds, of which *D. discoideum* is the best known example, the cells undergo two stages of differentiation. The first is a preliminary step which has been characterized both cytologically and biochemically (see MacWilliams & Bonner 1979; Morrissey 1982 for reviews). It partitions the slug into a group of cells in the anterior region that will become stalk cells, the prestalk cells, and a larger group of cells in the posterior region that will ultimately become spores, the prespore cells. In the second stage of differentiation, during culmination, the prestalk cells enlarge, vacuolate, and die. They do this just as they enter the tip of the cellulose stalk that they themselves secreted before they died. The prespore cells are lifted into the air passively; early in culmination the prespore amoebae become individually encapsulated in elliptical cellulose cases. The moment this encapsulation occurs it is clear that the remaining upward movement of the fruiting body has to be achieved by the prestalk cells for they are the only remaining motile cells.

Bonner (1944) showed that spore encapsulation occurred when the length of the mass of spore and prestalk cells climbing the stalk equalled the length of stalk visible beneath it. Thus only a very small fraction of the total stalk erection process had occurred when the spore cells became mechanically passive. Measurement of the speed at which the cell mass climbed the stalk during the entire culmination process showed no decrease whatever in this climbing speed at the time when spore encapsulation occurred (Bonner & Eldredge 1945). This experiment shows that removing whatever motive force the spore cells may contribute does not perceptibly diminish the motive force of the entire cell mass during culmination.

Since the pioneering experiments of Raper (1940), it has been understood that each of these preliminary prestalk and prespore types must convert into the other; they are labile differentiation states. He showed that if a slug was cut into segments perpendicular to its long axis, then the anterior prestalk cell segment produced both stalk and spore cells, and the same was true of an isolated segment of posterior prespore cells. While there has never been any doubt that the two cell types interconvert, questions have remained about the speed at which interconversion can occur.

Raper showed that isolated posterior segments regulated rapidly (that is, regenerated prestalk and prespore types in the proper 30–70 % ratio), while the anterior segments took many hours to regulate. This has been interpreted to mean that prestalk cells convert to prespore cells slowly, but the reverse conversion can be rapid. These differences in the rates of conversion were supported by experiments of many authors, including Gregg (1965) and Sakai (1973). More recently Gregg & Davis (1982) have shown that the conversion from prespore to prestalk

can be very rapid, taking only a few minutes to occur. There is, however, a complication, for Sternfeld & David (1981) have evidence that 'anterior-like' cells always inhabit the posterior prespore region, and they suggest that there has not been a massive interconversion of cells in isolated posterior segments of slugs, but that these anterior-like cells are dormant prestalk cells that simply move forward and become the new prestalk zone.

A possible difficulty with all these regulation experiments in chopped up segments of grexes is that they do not necessarily reflect what is happening in normal intact slugs. If, however, the slow (many hour) prestalk–prespore conversion time deduced from them is accurate in intact slugs, then the simplest form of our model cannot be quantitatively accurate. That simplest form can account for the preliminary labile prestalk–prespore differentiation by having cells continuously circulate through a standing axial chemical gradient. The anterior chemical conditions induce prestalk behaviour while the posterior environment induces prespore behaviour. To propel a grex at the approximate speed of one grex length per hour, the cell fountain our model predicts must circulate about once per hour, and this means a typical cell must convert between prestalk and prespore identity about once per hour. If this timing is impossible, then we would have to include in our model true cell heterogeneity, that is, distinct subpopulations of cells. Then, for example, the proposed circulation of cells might only take place in the anterior, prestalk zone. This idea is not inconsistent with some other experimental findings that we will cite below.

Finally, we discuss a caution concerning vital dyes, such as neutral red. These have provided convenient ways of identifying the prestalk and prespore zones (Bonner 1952). But the staining difference between the two zones is probably due to a difference in the pH in the lysosomal vacuoles (Tasaka & Takeuchi 1983) and therefore, if a cell does convert, it presumably changes its colour (prestalk is dark; prespore is faintly stained). For this reason, movement of coloured cells marked by vital dyes may be misleading, as the cells may slowly change colour as they move anteriorly or posteriorly. This is merely postulated, because if dark red anterior cells are grafted into the posterior region they do not lose their colour quickly. Furthermore, Sternfeld & David (1981) have evidence that the dye is stable for very long periods in individual cells.

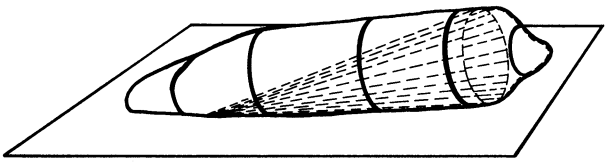

FIGURE 12. Schematic of the dye concentration region seen in figure 11. From side views, we know the central dye core lies close to the agar floor and far from the upper surface of the grex. The dye region is roughly cone-shaped, as indicated by the dashed lines.

Regardless of the exact cell property indicated by neutral red dye, we suggest that the boundary between darkly and lightly stained regions in migrating grexes is not always a sharply defined surface perpendicular to the axis of the grex. In figure 11, plate 2, we show colour photographs of several stained grexes comprising cells uniformly exposed in suspension to neutral red dye before plating on agar. They are migrating freely and showing, much more often than not, a reddish tip with a distinct river of red cells running back to the tail.

PHILOSOPHICAL TRANSACTIONS OF THE ROYAL SOCIETY B BIOLOGICAL SCIENCES

We believe the cells that show their colours most brightly are concentrated in a cone-shaped region with its base at the grex tip and its apex near the tail touching the agar floor. This is indicated schematically in figure 12.

6.2. *Movement of cell clumps grafted into a grex*

As discussed above, many studies show anterior red cells placed in the posterior region migrate as a clump towards the anterior end of a slug (see, for example, Bonner 1952; Yamamoto 1977). Furthermore, less intensely stained red posterior cells, transplanted to the anterior prestalk region, will move as a block of cells posteriorly. Therefore, transplanted groups of cells tend to return to their original position. Conversely, cells from any position, grafted to the corresponding position of another slug often tend to remain in that homologous position.

These results would seem to contradict the vital dye experiments described in §3, especially that shown in figure 5*b*. Note, however, that in the imprisoned grex in figure 5*a*, while some of the transplanted posterior red cells streak rapidly to the anterior end, most remain in the posterior end for at least 1 h. A possible resolution of the apparent contradiction is that two separate processes are taking place. First, a certain degree of differentiation delineates the two major zones in the slug. And, though labile on a time scale of hours, this differentiation acts to 'attract' cells, displaced surgically to a different zone, back toward their original position, even while those cells slowly lose their previous differentiation commitment. Second, superimposed on a general tendency for the prestalk and prespore zones to maintain their integrity, there is much rapid circulatory movement within each zone. With the demarcation between the prestalk and prespore zones diffuse and labile, there is some degree of mixing between the two zones. This may be reflected in continuous posterior–anterior and anterior–posterior cell plumes and these may be especially vigorous in an imprisoned grex. That cells percolate through a slug from one zone to another is shown clearly in the grafting experiments of Bonner & Adams (1958) and in the slug reversal experiments of Yamamoto (1977).

There is convincing evidence for pronounced continuous cell circulation in the anterior prestalk zone. Speigel (1983 and personal communication) has observed, tracking individual cells by using Nomarski optics, that there is a continuous reverse fountain of cell movement in the anterior end of *D. discoideum* migrating slugs. H. K. MacWilliams (personal communication) has done some grafts inwhich he has stained the anterior half of the prestalk zone with neutral red and the posterior half with Nile blue sulphate. After the slugs migrate for some time, he finds a central column of red cells penetrating back though the centre of the blue cells, providing further evidence for a reverse fountain. By digitizing the position of individual vitally stained cells in successive frames of time-lapse movies, Durston & Vork (1979) have demonstrated the existence of large diameter vortices in prestalk zones of some slugs. Clark & Steck (1979) report helical motion of cells in a slug and propose this can move the slug.

Several experimental studies support the view that the most intense cell circulation and most of the motive force production is concentrated in the anterior prestalk zone, and that the posterior prespore zone is carried along as passive baggage. In an important study, Inouye & Takeuchi (1979, 1980) have directly measured the pressure head needed to stall segments of a grex induced to migrate inside a cylindrical agar tunnel. (See also Inouye (1984).) In this way, they have shown motive force competence to be concentrated in the anterior end. By using time-lapse videotape movies, we have observed in a slug imprisoned in agar that, after a recovery period, the cells in the anterior third churn about violently, while those in the posterior end

PHILOSOPHICAL TRANSACTIONS OF THE ROYAL SOCIETY B BIOLOGICAL SCIENCES

remain nearly passive (unpublished result). Another piece of evidence is that during culmination, as mentioned previously, the prespore cells turn into non-motile spores at a relatively early stage, so the upward motion of the majority of culmination is entirely the result of the reverse fountain activity of the prestalk region. Finally, in a series of most interesting observations, Francis (1959, 1962) has provided evidence that the anterior cells of the slug move more rapidly than do the posterior cells. All of these facts are consistent with the idea that our model applies more to the anterior zone than to the prespore region.

When Inouye & Takeuchi (1980) observed the shape of the tip of the grex they stalled in a tube by elevating the anterior pressure, they found it to be convex outward. If only the cells touching the periphery were contributing motive force, carrying the interior cells along as passive baggage, then they should have seen a concave tip shape. Their observation indicates that all cells in some cross-sections of the grex are contributing motive force. The streamlines in the reverse fountain flow our model predicts in an imprisoned grex (see figure 4) could be naively interpreted to cause a concave tip shape, so we emphasize that the opposite is true. The cell fountain is reversed because the agar prison walls can sustain (without noticeably deforming) any force needed to push the core cells backward. In our model the hydrostatic pressure is highest at the anterior tip and this should lead to a convex tip shape as observed by Inouye & Takeuchi when a grex is stalled by imposed hydrostatic pressure instead of a rigid flat wall.

6.3. *Chemotaxis and orientation of cells in the grex*

It has been known for a long time that the cells inside the migrating slug and in the culminating cell mass have clear-cut non-random orientations (see Bonner 1944; Shaffer 1962, 1964). In general, the orientation in the anterior end, which is especially obvious during culmination, shows many cells oriented at right angles to the long axis of the slug. Usually the posterior cells appear more isodiametric. However, in a recent unpublished scanning electron microscope study, Smith (1983) has shown that often the cells in the posterior end are oriented with their long axes parallel to the slug axis. Kopachick (1982) has splendid SEM micrographs which make clear that, in the beginning of slug formation, cell orientation is very similar to what one finds during aggregation.

There has been increasing evidence that justifies thinking that cell chemotaxis occurs within the slug. This was first put forward in an early thesis of David Francis (1959), and fortified with compelling evidence by Matsukuma & Durston (1979). More recently Sternfeld & David (1981) have shown that, if small masses of slug cells are encased in agar, external cyclic AMP will cause prestalk and prespore cells to sort out within the enclosed ball of cells. They also showed that oxygen gradients had a chemotactic effect on cells within the ball, which is consistent with Yamamoto's (1977) polarity reversal of slugs in dead-end agar tunnels.

From all these observations it is presumed that cyclic AMP gradients operate not only during aggregation but also in the same fashion during slug migration. In aggregation, streams form in which the cells are elongate and attached end to end. The cyclic AMP in such streams acts in a pulse relay system from cell to cell. This requires a pacemaker to initiate pulses at the centre or tip, and chemotactic movement toward the apparent cyclic AMP source to occur in waves which originate at the pacemaker. If individual cells are stimulated by a tiny drop of cyclic AMP from a micropipette, they will put out pseudopods and elongate in the direction of higher concentrations of cyclic AMP (Gerisch *et al.* 1975; Swanson & Taylor 1982). If the cells are attached in a stream, then it is only the anterior cells on the stream that *can* respond to an

PHILOSOPHICAL TRANSACTIONS OF THE ROYAL SOCIETY B BIOLOGICAL SCIENCES

acrasin gradient (Shaffer 1962, 1964). The tip is not only the pacemaker, but also secretes the highest concentrations of cyclic AMP. There is evidence for overall gradients of cyclic AMP in the slug (Bonner 1949; Pan *et al.* 1972; Rubin & Robertson 1975; Brenner 1977; Schaap & Wang 1984).

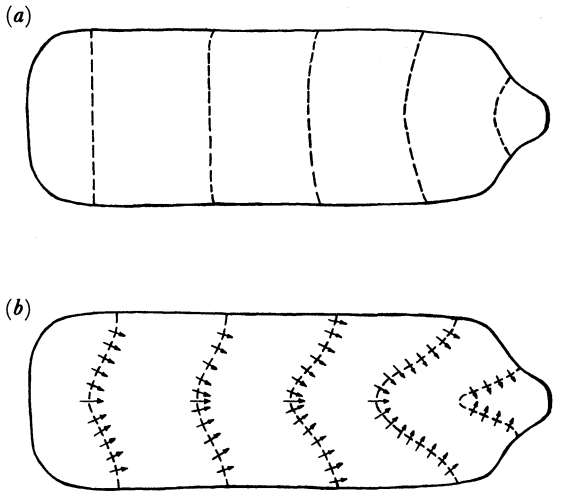

FIGURE 13. Dashed lines in (*a*) show expected cAMP fronts when there is no convection of the cAMP field by cell motion. Except for a region close to the tip, these fronts are nearly perpendicular to the slug axis. Therefore, the cell orientation we propose, steered by the cAMP gradient, would be parallel to the axis of the slug.

Dashed lines in (*b*) show how we expect convection (at velocity w, defined in §4.1) associated with a general reverse fountain flow of cells shown in figure 2*a* to warp the cAMP front loci. The short line segments with arrows show the corresponding cell orientation up the cAMP gradient. Qualitatively, the cell orientation field shown corresponds well to that observed experimentally. We have not yet solved the free boundary problem corresponding to a freely migrating grex, so this figure is conjecture based on the simple boundary value problem we did solve (described in §2.3).

In our model, cell orientation is aimed by the cyclic AMP gradient. If no cell circulation occurred within the slug, then constant cyclic AMP fronts would be roughly perpendicular to the long axis of the slug as shown in figure 13*a*. Cell orientation perpendicular to these fronts, thus parallel to the slug's long axis, would be consistent with that observed in the posterior region of the slug, but would not match the orientation seen in the prestalk region. The reverse fountain flow of cells, however, convects cyclic AMP and warps the constant cyclic AMP fronts into the configuration shown qualitatively in figure 13*b*. Near the tip, orientation perpendicular to these fronts points almost radially toward the slug axis as is observed. This effect occurs (but is not shown graphically) in the simple simulations depicted in figure 2. We have not solved the free boundary value problem appropriate in the case of a freely migrating grex and so we cannot announce the cell orientation our model will predict. But, qualitatively, we expect it to be consistent with the observed orientation.

6.4. *Chemotaxis of the entire slug*

It has been known for some time that grexes rising up into the air are oriented by a gas that they themselves secrete (Bonner & Dodd 1962). The gas is a repellent. If two fruiting bodies rise close together, each repels the other and they veer apart. If a fruiting body rises near an agar wall, it veers away from the wall (see figure 14*a*).

PHILOSOPHICAL TRANSACTIONS OF THE ROYAL SOCIETY B BIOLOGICAL SCIENCES

If the culminating grex finds itself close to a vertical wall, then this evaporating repellent gas will have a higher concentration next to the wall. Although the detailed fashion in which the repellent gas acts is not yet known, it could work by inducing the cells experiencing the highest repellent concentration to move fastest. To see this, consider if, in a rank of soldiers marching north while maintaining a constant lateral separation, those to the east march faster than those to the west, the result is to bend the direction in which each rank moves to the west. Geometrical optics provides an alternative metaphor: refraction bends light wavefronts toward regions wherein light rays move more slowly. If, as shown in figure 14*b*, higher concentrations of the repellent chemical cause cells to crawl faster, cells adjacent to the wall will crawl faster than cells opposite the wall. The expected result is that the upward trajectory of the grex and the stalk it climbs will veer away from the wall.

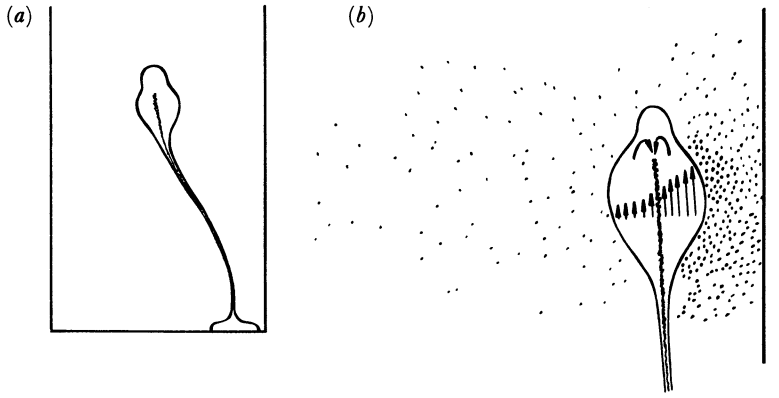

FIGURE 14. (*a*) The way a fruiting body bends its stalk to centre the spore sack in a cave. In (*b*), dots show gas molecules which evaporate from the grex and concentrate near a wall acting as a barrier to diffusion of the gas. The gas, thought to be a 'repellent', could act by making amoebae that see higher concentrations of it crawl faster as shown by the vertical arrows. This should cause the fruiting body to deflect away from the wall.

We emphasize this important general point: a chemical that acts to increase crawling speed will seem to repel a crawling group of cells. The repellent that acts to make climbing grexes veer away from each other and from walls may act this way, and would then have exactly the property our hypothetical ζ needs.

6.5. *The search for the 'other' chemical*

Recently Bonner *et al.* (1985) have shown that slugs can sense a pH gradient in the agar substratum. If there is a significant pH gradient, then slugs will migrate towards the acid side. In that paper we pointed out that since high pH will favour a high NH_3/NH_4 ratio, the slugs might be moving away from high concentrations of NH_3. This is perhaps a clue about the identity of the orienting gas in our earlier experiments. Should this be the case, then NH_3 would be a logical candidate for ζ; this substance is known to be produced continuously by cells in the grex.

Williams *et al.* (1984) show that NH_4Cl modulates cAMP relay competence in *D. discoideum*, so, if ammonia is ζ, then it will have an indirect effect upon cAMP kinetics that we have not modelled. McConaghy *et al.* (1984) demonstrate that in *D. discoideum* NH_3 reversibly inhibits

cell–cell cohesion during the aggregation phase. Any chemical that modulates cell–cell cohesion would have an apparent chemokinesis effect. Unfortunately, different cohesion mechanisms are active during aggregation and slug morphogenesis, and the latter is not sensitive to ammonia according to these authors.

Fisher *et al.* (1983) have discovered and studied a chemical they called slug turning factor (STF) (see also Fisher *et al.* 1981). Migrating grexes deflect away from concentrated patches of STF and therefore it is another possible candidate for ζ.

7. Summary and conclusions

How the cellular slime mould grex moves is an important and longstanding scientific puzzle, as is the issue of orientation of cells in the grex: orientation that is often, as in the case of culminating cell masses, in quite a different direction from the overall movement of the grex. A valid explanation of these phenomena will mark a crucial step toward understanding how, through interaction among many identical simple cells, complex behaviour at the organismic level results. We feel that each of the previous speculative solutions of these puzzles, suggested by many workers, has serious defects.

With this paper we provide a mathematical model with a sound theoretical basis in classical continuum mechanics, whose underlying assumptions are supported by both past and current experimental results of many workers, and whose preliminary predictions are confirmed by new experiments reported here. In the simplest terms, our model assumes existence and maintenance of two standing chemical gradients: first, an axial acrasin gradient, highest at the tip and progressively lower as one proceeds down the main axis of the grex, and second, a radial gradient of a chemokinesis chemical (yet to be identified), highest along the central axis and lowest at the surface of the grex. The first (acrasin) gradient orients each cell's aim toward the apparent source of the chemoattractant, while the second (chemokinesis) chemical modulates the traction each cell exerts upon its neighbours. Each cell within the grex moves relative to its neighbours by amoeboid crawling. The two chemical gradients cause some of the cells to push forward within the grex at the expense of others that are pushed backward in a reverse fountain flow, as seen in a coordinate system attached to the tip of the grex. This motion of the individual cells, guided and controlled by the two gradients, results in the overall movement of the grex, both during the migration phase when it is stalkless, and during the culmination phase when it rises on a stiff central stalk.

Our paper, too, includes a substantial measure of speculation. On the one hand, our mathematical analysis (see §4.2) forces us to assume existence of the second chemokinesis chemical and 'contaminate' our model's foundation with a hypothetical 'morphogen'. On the other hand, we have offered conjectures on how we expect yet-to-be-computed solutions to our formidable nonlinear partial differential equations to behave (in §§2.4, 2.5, and 2.6). Neither speculation is idle; each is subject to direct experimental falsification or verification. Our hypothetical chemokinesis factor should be possible to identify because its hypothesized traction modulation effects can be observed directly. The exact behaviour of our partial differential equation model in the contexts outlined in §§2.4, 2.5, and 2.6 can be determined simply by doing the 'computer experiments' of solving the appropriate equations numerically. Each of these experimental quests is underway, but each is very difficult, so we believe publication of our results in the present preliminary form is justified.

PHILOSOPHICAL TRANSACTIONS OF THE ROYAL SOCIETY B BIOLOGICAL SCIENCES

The greatest conflict between our new model and earlier experiments is that the line of demarcation between the anterior prestalk zone and the posterior prespore zone has been thought to remain sharp for many hours during migration. There is evidence in older grexes, where such a regional early differentiation is well established, and in culminating grexes where the prespore–prestalk difference is even more marked, that the anterior prestalk zone is largely responsible for the overall movement. The prespore cells are mostly dragged along passively. In §1 we explained how, ultimately, the slug should be viewed as a mixture of two subpopulations, each percolating through the other and interconverting into the other. We expect our model to characterize the behaviour of the prestalk subpopulation, but, for conceptual simplicity, we ignored the prestalk–prespore difference in the mathematical modelling process.

The virtue of our model is that it not only provides a much-needed explanation for grex movement, but it may also account for numerous associated phenomena. These include cell orientation within the slug, tip (and even multiple tip) formation and slug elongation at the end of aggregation, maintenance of the tip and the geometrical aspect ratio throughout development, and steerage of the whole grex.

G.M.O. gratefully acknowledges the financial support from a Guggenheim Fellowship, the Science and Engineering Research Council of Great Britain through grant GR/C/63595, and National Science Foundation grant number MCS 83-01460. Work by J.T.B. was partly supported by National Science Foundation grant number PCM-8202442 and by the American Cancer Society grant number CD-186. G.M.O. thanks the Centre for Mathematical Biology of the Mathematical Institute at the University of Oxford for generously extending hospitality and use of facilities.

We thank Hannah Suthers for expert assistance with some of the experiments described, for doing others single-handedly, and for help with the manuscript.

Harry MacWilliams not only shared unpublished experimental results (§6.2) with us, but also offered significant criticism of an early draft. He stimulated the addition of §3.6. Peter Newell, Anthony Durston, and Keith Williams made helpful biological suggestions.

We acknowledge many useful suggestions and helpful criticisms concerning mathematical modelling aspects contributed by Edward Cox, George Oster, Lee Segel and Arthur Winfree. Fred Spiegel communicated results of important experiments on cell trajectories before publishing them.

Alan Goldfarb, Karen Odell and Holly Elizabeth Rowe transformed many segments of originally opaque language into lucid ones.

References

Bonner, J. T. 1944 A descriptive study of the development of the slime mold *Dictyostelium discoideum*. *Am. J. Bot.* **31**, 175–182.

Bonner, J. T. 1949 The demonstration of acrasin in the later stages of the development of the slime mold *Dictyostelium discoideum*. *J. exp. Zool.* **110**, 259–271.

Bonner, J. T. 1952 The pattern of differentiation in amoeboid slime molds. *Am. Nat.* **86**, 79–89.

Bonner, J. T. & Eldredge, E. D. 1945 A note on the rate of morphogenetic movement in the slime mold *Dictyostelium discoideum*. *Growth* **9**, 287–297.

Bonner, J. T. & Adams, M. S. 1958 Cell mixtures of different species and strains of cellular slime molds. *J. Embryol. exp. Morph.* **6**, 346–355.

PHILOSOPHICAL TRANSACTIONS OF THE ROYAL SOCIETY B BIOLOGICAL SCIENCES

Bonner, J. T. & Dodd, M. R. 1962 Evidence for gas-induced orientation in the cellular slime molds. *Devl Biol.* **5**, 344–361.
Bonner, J. T., Hay, A., John, D. G. & Suthers, H. B. 1985 pH affects fruiting and slug orientation in *Dictyostelium discoideum*. *J. Embryol. exp. Morph.* **87**, 207–213.
Brenner, M. 1977 Cyclic AMP gradient in migrating pseudoplasmodia of the cellular slime mold *Dictyostelium discoideum*. *Devl Biol.* **252**, 4037–4077.
Clark, R. L. & Steck, T. L. 1979 Morphogenesis in *Dictyostelium*: an orbital hypothesis. *Science, Wash.* **204**, 4398, 1163–1167.
Durston, A. J. & Vork, F. 1979 A cinematographical study of the development of vitally stained *Dictyostelium discoideum*. *J. Cell Sci.* **36**, 261–279.
Finlayson, B. A. & Scriven, L. E. 1969 Convective instability by active stress. *Proc. R. Soc. Lond.* A **310**, 183–219.
Fisher, P. R., Grant, W. N., Dohrmann, U. & Williams, K. L. 1983 Spontaneous turning behavior by *Dictyostelium discoideum* slugs. *J. Cell Sci.* **62**, 161–170.
Fisher, P. R., Smith, E. & Williams, K. L. 1981 An extracellular chemical signal controlling phototactic behavior by *Dictyostelium discoideum* slugs. *Cell* **23**, 799–807.
Francis, D. W. 1959 Pseudioplasmodial movement in *Dictyostelium discoideum*. Master's dissertation, University of Wisconsin.
Francis, D. W. 1962 The movement of pseudoplasmodia of *Dictyostelium discoideum*. Ph.D. dissertation, University of Wisconsin.
Gerisch, G., Hulser, D., Malchow, D. & Wick, U. 1975 Cell communication by periodic cyclic-AMP pulses. *Phil. Trans. R. Soc. Lond.* B **272**, 181–192.
Goldbeter, A. & Segel, L. A. 1977 Unified mechanism for relay and oscillation of cyclic AMP in *Dictyostelium discoideum*. *Proc. natn. Acad. Sci. U.S.A.* **74**, 1543–1547.
Gregg, J. H. 1965 Regulation in the cellular slime molds. *Devl Biol.* **12**, 377–393.
Gregg, J. H. & Davis, R. W. 1982 Dynamics of cell redifferentiation in *Dictyostelium mucoroides Differentiation* **21**, 200–204.
Harris, A. K. 1973 Cell surface movements related to cell locomotion. In *Locomotion of tissue cells* (ed. R. Porter & D. W. Fitzsimons), Ciba Foundation Symposium 14 (new series), p. 3. Amsterdam: Elsevier/North Holland.
Inouye, K. 1984 Measurement of the motive force of the migrating slug of *Dictyostelium discoideum* by a centrifuge method. *Protoplasma* **121**, 171–177.
Inouye, K. & Takeuchi, I. 1979 Motive force of the migrating pseudoplasmodium of the cellular slime mold *Dictyostelium discoideum*. *J. Cell Sci.* **41**, 53–63.
Inouye, K. & Takeuchi, I. 1980 Analytical studies on migrating movement of the pseudoplasmodium of *Dictyostelium discoideum*. *Protoplasma* **99**, 289–304.
Keller, E. F. & Segel, L. A. 1970 Initiation of slime mold aggregation viewed as an instability. *J. theor. Biol.* **26**, 399–415.
Kopachik, W. 1982 Orientation of cells during slug formation in *Dictyostelium*. *Wilhelm Roux Arch. Devl Biol.* **191**, 348–354.
MacKay, S. A. 1977 Computer simulation of aggregation in *Dictyostelium discoideum*. *J. Cell Sci.* **33**, 1–16.
MacWilliams, H. K. & Bonner, J. T. 1979 The prestalk–prespore pattern in cellular slime molds. *Differentiation* **14**, 1–22.
Matsukuma, S. & Durston, A. J. 1979 Chemotactic cell sorting in *Dictyostelium discoideum*. *J. Embryol. exp. Morph.* **50**, 243–251.
McConaghy, J. R., Saxe III, C. L., Williams, G. B. & Sussman, M. 1984 Reversible inhibition of aggregation-related cohesivity in *Dictyostelium discoideum* by diffusible metabolites. *Devl Biol.* **105**, 389–395.
Morrissey, J. H. 1982 Cell proportioning and pattern formation. In *The development of Dictyostelium discoideum*, pp. 411–449. New York and London: Academic Press.
Pan, P., Hall, E. M. & Bonner, J. T. 1972 Folic acid as a second chemotactic substance in the cellular slime moulds. *Nature, new Biol.* **237**, 181–182.
Parnas, H. & Segel, L. A. 1978 A computer simulation of pulsatile aggregation in *Dictyostelium discoideum*. *J. theor. Biol.* **71**, 185–207.
Raper, K. B. 1940 Pseudoplasmodium formation and organization in *Dictyostelium discoideum*. *J. Elisha Mitchell Sci. Soc.* **56**, 241–282.
Rubin, J. & Robertson, A. 1975 The tip on the *Dictyostelium discoideum* pseudoplasmodium as an organizer. *J. Embryol. exp. Morph.* **33**, 227–241.
Sakai, Y. 1973 Cell type conversion in isolated prestalk and prespore fragments of the cellular slime mold *Dictyostelium discoideum*. *Devl Growth Diff.* **15**, 11–19.
Schaap, P. & Wang, M. 1984 The possible involvement of oscillatory cAMP signalling in multicellular morphogenesis of the cellular slime molds. *Devl Biol.* **105**, 470–478.
Segel, L. A. 1984 *Modelling dynamic phenomena in molecular and cellular biology*, chapter 6. Cambridge University Press.
Shaffer, B. M. 1957 Aspects of aggregation in cellular slime molds. I. Orientation and chemotaxis. *Am. Nat.* **91**, 19–35.
Shaffer, B. M. 1962 The Acrasina. *Adv. Morphogenesis* **2**, 109–182.

PHILOSOPHICAL TRANSACTIONS OF THE ROYAL SOCIETY B BIOLOGICAL SCIENCES

Shaffer, B. M. 1964 The Acrasina II. *Adv. Morphogenesis* **3**, 301–322.
Smith, B. N., Jr 1983 Cell orientation and movement in the migrating pseudoplasmodium of *Dictyostelium discoideum*. A.B. thesis, Princeton University.
Spiegel, F. 1983 Morphological differentiation of prestalk cells in migrating slugs of *Dictyostelium discoideum*. *J. Cell Biol.* **97**, 58A.
Sternfeld, J. & David, C. N. 1981 Cell sorting during pattern formation in *Dictyostelium*. *Differentiation* **20**, 10–21.
Swanson, J. A. & Taylor, D. L. 1982 Local and spatially coordinated movements in *Dictyostelium discoideum* amoebae during chemotaxis. *Cell* **28**, 225–232.
Tasaka, M. & Takeuchi, I. 1983 Cell patterning during migration and early culmination in *Dictyostelium discoideum*. *Differentiation* **23**, 184–188.
Williams, G. B., Elder, E. M. & Sussman, M. 1984 Modulation of the cAMP Relay in *Dictyostelium discoideum* by ammonia and other metabolites: possible morphogenetic consequences. *Devl Biol.* **105**, 377–388.
Yamamoto, M. 1977 Some aspects of behavior of the migrating slug of the cellular slime mold *Dictyostelium discoideum*. *Devl Growth Diff.* **19**, 93–102.

PHILOSOPHICAL TRANSACTIONS OF THE ROYAL SOCIETY B BIOLOGICAL SCIENCES

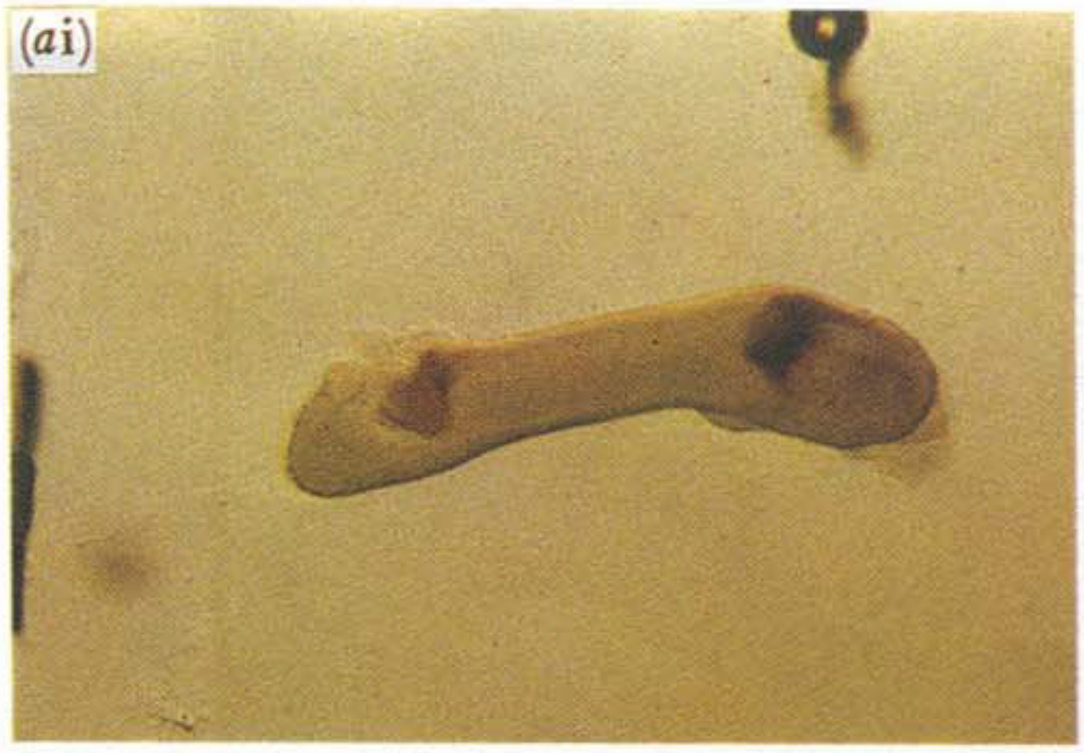

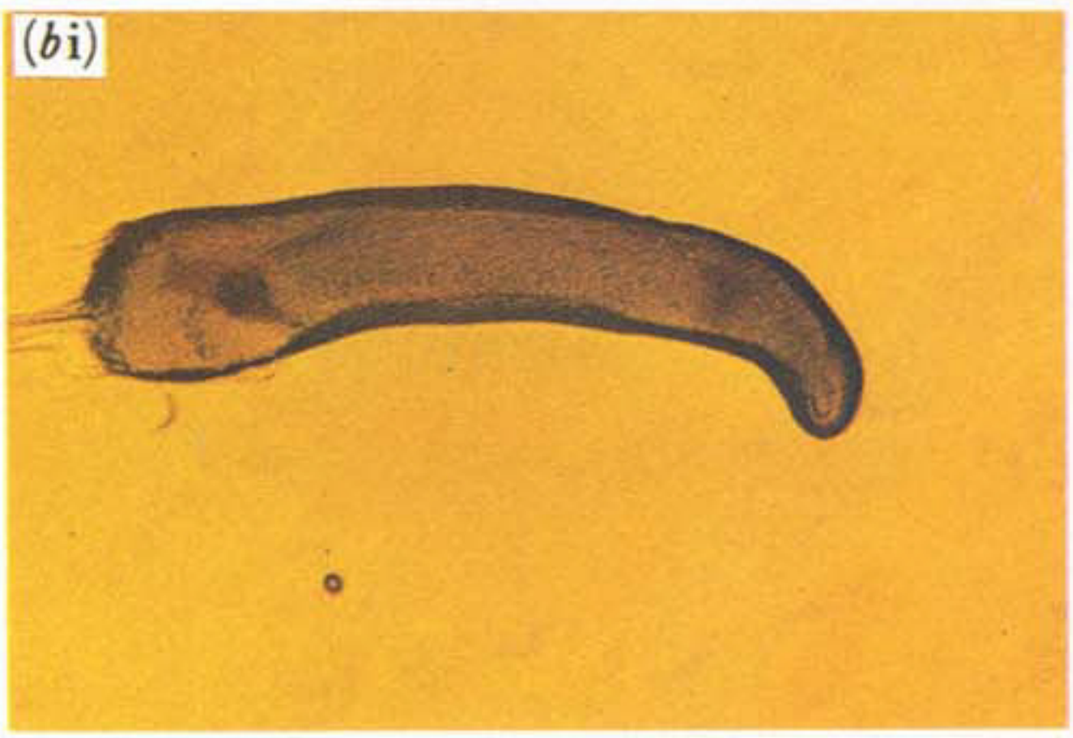

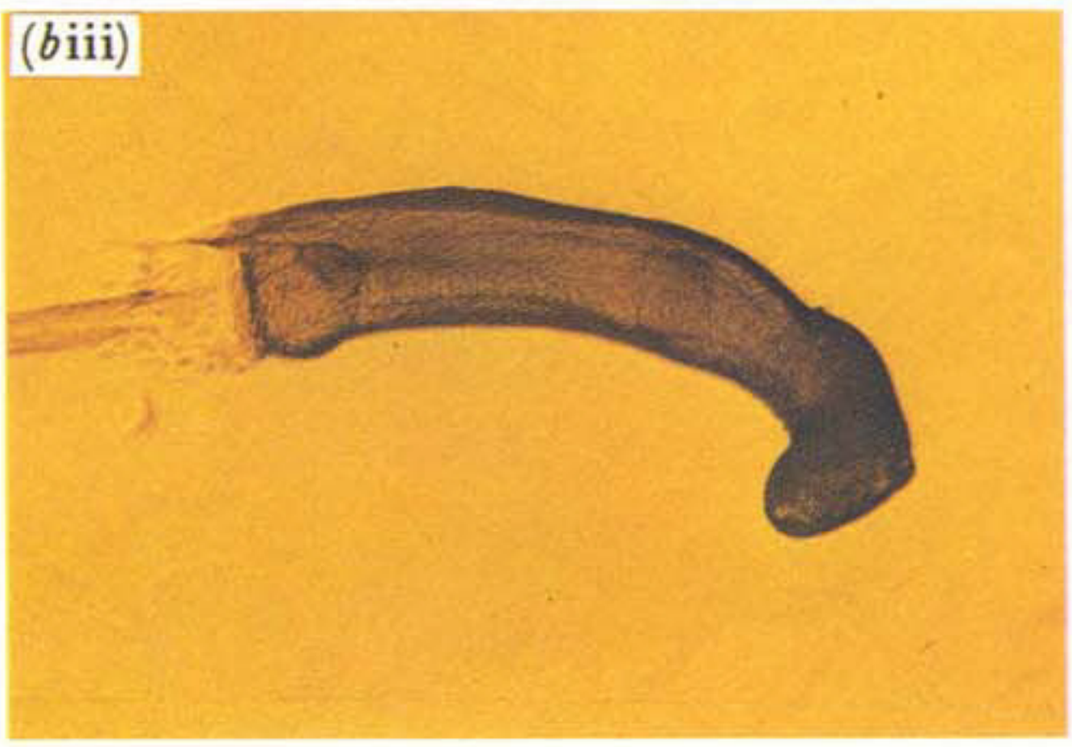

PHILOSOPHICAL TRANSACTIONS OF THE ROYAL SOCIETY B BIOLOGICAL SCIENCES

FIGURE 5. For description see opposite.

(*Facing p.* 500)

FIGURE 11. Top view photographs of free-crawling grexes, stained with neutral red dye. Note the dye concentration extending in a central river back from the tip. This persists until culmination.